Whole genome regulatory effect of *MoISW2* and consequences for the evolution of the rice plant pathogenic fungus *Magnaporthe oryzae*

Mengtian Pei[1*], Yakubu Saddeeq Abubakar[2,3], Hina Ali[1], Lianyu Lin[1], Xianying Dou[1], Guodong Lu[1], Zonghua Wang[1,4], Stefan Olsson[1,5*#], Ya Li[1#]

[1]State Key Laboratory of Ecological Pest Control for Fujian and Taiwan Crops, College of Plant Protection, Fujian Agriculture and Forestry University, Fuzhou 350002, China

[2]Key Laboratory for Plant-microbe Interaction, College of Life Sciences, Fujian Agriculture and Forestry University, Fuzhou 350002, China

[3]Department of Biochemistry, Faculty of Life Sciences, Ahmadu Bello University, Zaria 810103, Nigeria

[4]Institute of Oceanography, Minjiang University, Fuzhou, China

[5]Synthetic Biology Center, College of Future Technologies, Fujian Agriculture and Forestry University, Fuzhou 350002, China

*First authors Mengtian Pei and Stefan Olsson

#Corresponding authors:

Ya Li and Stefan Olsson

liya-81@163.com & Stefan@olssonstefan.com

Author contributions:

Mengtian Pei: ChIPseq and initial analyses; RNAseq and initial analyses; manuscript preparation and writing.

Yakubu Saddeq Abubakar: Constructive manuscript critique; manuscript corrections

Hina Ali: ChPseq; RNAseq

Lianyu Lin: Retrotransposon analysis of ChPseq data.

Xianying Dou: Constructive manuscript critique; manuscript corrections

Guodong Lu: Supervision; manuscript corrections

Zonghua Wang: Supervision; manuscript corrections

Ya Li: Obtaining funds; supervision; initial planning of experiments; construction of ISW2 mutant and phenotype analysis; manuscript preparation and writing

Stefan Olsson: ChIPseq and RNAseq extended analyses and synthesis; MEME, FungiFun, antiSMASH analyses; manuscript planning; manuscript preparation and writing.

Keywords: heterochromatin, epigenetics, nucleosomes, avirulence genes, retrotransposons, evolution

Abstract

Isw2 proteins are conserved in eukaryotes and are known to bind to DNA and dynamically influence local chromosome condensation close to their DNA binding site in an ATP-dependent manner making genes close to the binding sites more accessible for transcription and repression. A putative *MoISW2* gene was deleted with large effects on plant pathogenicity as a result. The gene was complemented and a ChIP-sec was performed to identify binding sites. RNAsec showed effects on the overall regulation of genes along the chromosomes for mutant and background strains and this was compared with RNAseq from 55 downloaded RNA-seq datasets from the same strain and found similar. MoIsw2 binding and activities create genomic regions affected by MoIsw2 with high gene expression variability close to the MoIsw2 binding sites while surrounding regions have lower gene expression variability. The genes affected by the MoIsw2 activity are niche-determinant genes (secreted proteins, secondary metabolites and stress-coping genes) and avirulence genes. We further show that MoIsw2 binding sites with the DNA binding motifs coincide with known transposable elements (TE) making it likely that TE-transposition at the binding sites can affect the transcription profile of *M. oryze* in a strain-specific manner. We conclude that MoIsw2 is a likely candidate for a master regulator, regulating the dynamic balance between biomass growth genes (like housekeeping genes) and nich-determinant genes important for ecological fitness. Stress-induced TE

63 transposition is together with MoIsw2 activity a likely mechanism creating more
64 mutations and faster evolution of the niche-determinant genes than for
65 housekeeping genes.

66

67

Introduction

The eukaryotic genome is organized into condensed nucleosomes, limiting access to DNA for transcription factors and more loosely packed regions that are easier to access for interactions with DNA for transcription factors and repressors. The cellular inheritance of this pattern is the basis of animal cell line specialization during embryogenesis (Serrano et al. 2013). Thus, DNA accessibility in fungi also plays an essential role in determining which genes can be efficiently transcribed (Huang et al. 2021).

Imitation Switch 2 (ISW2) belongs to the Imitation SWItch) subfamily (Uniprot) of the SNF2 (Sucrose__Non-Fermentable)/RAD54 helicase family. ISW2 proteins contain a Myb/Sant domain close to their C-termini that binds DNA. A role as a transcription factor is the main role often implicated for the Myb-domain containing family proteins in eukaryotes and especially in plants (Wieser and Adams 1995; Mateos et al. 2006; Du et al. 2009; Dubos et al. 2010; Lin et al. 2011; Lin et al. 2012; Prouse and Campbell 2012; Ambawat et al. 2013; Pattabiraman and Gonda 2013; Kim et al. 2014; Baldoni et al. 2015; Dong et al. 2015; Liu et al. 2015; Roy 2016; Matheis et al. 2017; Valsecchi et al. 2017; Verma et al. 2017; Allan and Espley 2018; Mitra 2018; Wang et al. 2018; J. Li et al. 2019; Ma and Constabel 2019; Cao et al. 2020; Li et al. 2024).

A true Isw2 should be involved in gene regulation by regulating the access to DNA for transcription factors and repressors through binding to DNA and controlling nucleosome positioning instead of being a classic transcription factor (TF) (Kagalwala et al. 2004; Fazzio et al. 2005; Hada et al. 2019). Generally, Isw2 proteins have a histone binding domain that interacts with histone 4 of a nucleosome and a catalytic ATPase domain close to the N-terminus that reacts with ATP and changes the Isw2 protein conformation (Whitehouse et al. 2007; Hota and Bartholomew 2011; Dang et al. 2014) so that the nucleosome moves towards the Isw2 DNA binding site (Fazzio et al. 2005), and in that way, transcription is regulated by changing TF and repressor proteins access to DNA. Isw2 is thus involved in targeted nucleosome positioning around these sites. As a consequence of this targeted positioning, a localized nucleosome condensation is created that negatively affects the regulation of the genes at the DNA binding site (Whitehouse et al. 2007) but favours regulation a bit further away from it (Fazzio et al. 2005; Donovan et al. 2021).

There has been much research into Isw2-like protein binding, but it has become clear that *in vitro* mapping of Isw2 binding and nucleosome positioning does not reflect what mechanistically occurs *in vivo* (Fazzio et al. 2005; Donovan et al. 2021), or the very transient nature of the interaction with His4 (Erdel et al. 2010; Erdel and Rippe 2011). The interaction is

transient in that the nucleosomes closest to the Isw2 binding sites get dynamically positioned by very frequent (seconds) interaction with the Isw2 protein in an ATP-dependent manner. The activity keeps the closest nucleosome(s) almost immobile, while nucleosomes further away get more freedom to move and genes there are easier to access and regulate. (Donovan et al. 2021). Experiments have shown that both the largest subunits of the Isw2 complex, Isw2, and Itc1, are needed for robust, target-specific binding to DNA while Isw2 alone is sufficient for basal-level binding (Fazzio et al. 2005).

Furthermore, Isw2 is known to bind DNA preferentially at intergenic regions (Whitehouse et al. 2007) where transposable elements (TEs) are commonly located (TE target sites). These sites are staggered cut palindromic target sites (Linheiro and Bergman 2008). In addition, TEs are involved in stress adaptation and host specialization in *Verticillium dahliae* (Faino et al. 2016) as well as in the rice blast fungus *Magnaporthe oryzae* studied here (Chadha and Sharma 2014; Yoshida et al. 2016) and should especially be needed when the host plant detects the fungus as a pathogen at the transition between the endophytic to necrotrophic infection phase of the fungus and thereafter (Cao et al. 2022).

ISW2 is highly expressed and often considered a "housekeeping" gene stably expressed under normal conditions (Machné and Murray 2012). The stable expression of housekeeping genes has recently been challenged, and many genes

130 traditionally considered stably expressed are unreliable when expressed outside
131 relatively narrow conditions. Thus better methods for selecting housekeeping
132 genes that better fit a specific set of conditions or tissues have been employed
133 (Stanton et al. 2017). On the other hand, the change in ratios of target genes to
134 housekeeping genes reflects the actual change in gene expression ratios of 2 genes
135 of interest. In a previous paper from our lab (Zhang, Zhang, Liu, et al. 2019), we
136 used correlations of expression profiles between genes of interest to probe
137 possible gene functions. That can be done in transcriptomic data from many labs
138 and is especially useful if the calculations are done for all data and not just average
139 value data. Then, also the variation between replicates can be used to calculate the
140 correlation between any two genes' expressions since these ratios reveal the
141 dependencies of one gene's expression on the other gene, or both genes'
142 expressions on a third. Using ratios of gene expressions can thus reveal putative
143 gene functions and help identify genes with specific putative functions that should
144 correlate with the expression of well-known orthologous genes (Zhang, Zhang, Liu,
145 et al. 2019).

146 In this study we studied the putative *MoISW2* in *M. oryzae* as an *ISW2*
147 gene that affects gene regulation close to the MoIsw2 protein binding sites in the
148 fungal genome. Deletion of the gene negatively affected pathogenicity and stress
149 tolerance. We further show that MoIsw2 binding is at TEs within the genome
150 and that genes close to the binding sites are more differentially regulated (up or
151 down). The affected genes are mainly niche-determinant genes; this, combined

with TE transpositions, is a likely mechanism for biased evolution (Monroe et al. 2022) in *M. oryzae* with a faster mutation rate for affected genes.

Results

Bioinformatics similarity and domain structure

The protein encoded by the MGG_01012 gene is annotated as a putative MoIsw2 in the NCBI database. From its N to C termini, Isw2 proteins consist of DExx, Helicase C, HAND, SANT and SLIDE domains (Hopfner et al. 2012) (Supplementary method 1 for further comparisons). Thus, the MoIsw2 protein is most probably an Isw2 protein of the IswI and Isw2 type (**Fig 1A)**

Deletion phenotypes of *ΔMoisw2* mutant and subcellular localization of the MoIsw2-GFP protein

The *MoISW2* gene was deleted in the *M. oryzae* Ku80 background strain and the deletion was confirmed by Southern blot (**Fig S1**). The effect of this mutation on the vegetative growth of the fungus was tested on three types of media namely complete medium (CM), minimal medium (MM) and rice bran medium (RBM), after incubation at 28 ℃ for ten days. The assays showed significantly decreased colony size of the mutant on all three

media when compared to the background strain Ku80 and the complemented strain (*ΔMoisw2*/*MoISW2*) (**Fig. 1B**).

A standard panel of stress treatments added to the CM medium was used to test whether the deletion of the *MoISW2* gene affected the fungal growth rates on different stressing media (Li et al. 2014). The CM medium without the addition of any stress-inducing agent was used as the control medium. The *ΔMoisw2* mutants are strongly inhibited by both SDS (affects membrane integrity) and NaCl (induces osmotic and ionic stress) compared to the controls (**Fig. 1C)**, suggesting that membrane pumps depending on the membrane potential might not be necessarily upregulated and working well in the mutant (Gostinčar et al. 2011).

Furthermore, we tested the ability of the mutant to produce conidia, which are essential for the spread of rice blast disease from plant to plant in the field. We tested this by checking the abundance of conidiophores (which bear conidia) in the various strains. While the WT and complemented strains produced many conidiophores, each bearing many conidia, the *ΔMoisw2* mutant only produced scanty conidiophores with very few conidia (**Fig. 1E**).

Next, the *ΔMoisw2* mutant was tested for pathogenicity on rice and barley leaves and compared with the Ku80 background strain and *ΔMoisw2*/*MoISW2* complemented strain**.** Since the *ΔMoisw2* mutant produces too few conidia to be used for inoculation, agar plugs were used

to infect healthy rice and barley leaves in the infection assay. The assay showed no infection for the *ΔMoisw2* mutant strains (**Fig. 1D**). We reasoned that this could be due to an inability of the mutant to penetrate the plant cuticles. Therefore, we inoculated the fungal strains on aseptically wounded leaves and found that the *ΔMoisw2* mutant could not develop any obvious disease symptoms on the leaves, indicating that *MoISW2* is needed for any successful infection of rice or barley leaves **(Fig. 1D**). From hyphae, *M. oryzae* can form appressoria needed for leaf infection. We found however that dark appressoria formation was not affected by the *MoISW2* mutation, confirming that the cause of no infection in the infection assay was probably not a complete lack of appressoria formation (**Fig. 1E**).

Finally, the Moisw2/*MoISW2-GFP* complementation was used to visualize the subcellular localization of MoIsw2. This was performed in a strain expressing Histon1-mCherry (RFP) (as a nuclear marker)(Zhang, Zhang, Chen, et al. 2019) because we expected that MoIsw2-GFP should accumulate in the nucleus as its orthologues do in other eucaryotes. The MoIsw2 protein was observed to consistently colocalize with the nuclear marker in hyphae, conidia and appressoria (**Fig. 1F**).

Taken together, these results suggest that MoIsw2 localize to nuclei and directly or indirectly regulates genes encoding proteins that in several ways strengthen the cell wall and cell membrane barrier important for

growth inside a plant and might explain why the deletion of the gene decreased the pathogenicity of the fungus.

Correlation analyses of *ISW2* expression with expressions of nucleosome histones and ITC1

Histone 1 (*HIS1* gene) is involved in epigenetic activities by changing access to DNA, and its expression is linked to silencing activity (Willcockson et al. 2021). The active Isw2 protein complex containing Itc1 binds DNA and Histone 4 (Donovan et al. 2021) also affects access to DNA. We used downloaded published expression data from the course of rice leaf infection from many experiments for the strain we use to investigate correlations between the putative *MoISW2* and the MoIsw2 complex gene candidates in the same way as we have done before for other genes using the same data (Zhang, Zhang, Liu, et al. 2019). We now investigate if the putative *MoISW2* is transcriptionally coregulated with genes that encode proteins MoIsw2 need to interact with to perform MoIsw2 local site-specific epigenetic activities. The *MoHIS1* expression increases steeply with *MoISW2* gene expression (**Fig. 2**). In *M. oryzae,* there are two genes (MGG_06293 and MGG_01160) *MoHIS4a* and *MoHIS4b* respectively that are predicted (NCBI) to encode an identical His4 protein. Thus the sum of these gene regulations should best reflect the regulation of the MoHis4 protein. Isw2 further works together with ITC1 in a complex that interacts with His4 (Kagalwala et al. 2004). Thus, the expression of these 4 putative genes (*MoISW2*, *MoITC1* and

MoHIS4a+MoHIS4b) producing 3 proteins (MoIsw2, MoItc1 and MoHis4) should be correlated in *M. oryzae,* and they are nicely correlated in the data from plant infection (**Fig. 2** and **Fig S2**). The closest correlation of *MoISW2* expression is even with *MoHIS4a+MoHIS4b.* Thus, it points to that the putative MoIsw2 is a real Isw2 as these proteins encoded by these genes are known to interact with His1, Itc1 and His4 in a complex (Fazzio et al. 2005). Furthermore, the expression of *MoHIS2B* is related to the overall growth rate (and thus *de novo* DNA synthesis rate) (Zhang, Zhang, Liu, et al. 2019) and is correlated with *MoISW2* but not with a steep slope. This points to that a smaller amount of MoHis2B is needed than His4 for handling the de novo DNA synthesis per cell than what is needed when Isw2 activity is high. That in turn could mean a lowering of the DNA-synthesis rate with higher *MoISW2* expression. Also, the expression of *MoHIS3* but not *MoHIS2A* is significantly correlated with the putative *MoISW2*. **(Fig. S3).** Although the MoIsw2 protein interacts directly with His4 according to the literature such interactions could not be detected using a yeast two-hybrid assay (data not shown) and the lack of positive results in this assay is likely due to the very transient nature of the interaction (Erdel et al. 2010; Erdel and Rippe 2011).

Thus, the putative *MoISW2* gene likely encodes a putative MoIsw2 protein involved in targeted local chromatin compaction working with MoHis1, MoItc1 and MoHis4 (Fazzio et al. 2005; Donovan et al. 2021; Willcockson et al. 2021). 2021). From now on, we skip “putative” as an attribute and investigate if MoIsw2

has the expected functions as an Isw2 and what other effects it has on the biology of the fungus. Furthermore, the local chromatin compaction and the regulatory effect caused by MoIsw2 should be dynamic and stronger the more the gene and the protein it encodes are expressed, and the more ATP there is available for the dynamic interaction.

ChIP-seq analysis of MoIsw2 finds DNA binding motifs

We made a MoIsw2-GFP fusion protein to perform a ChIP-seq analysis to find conserved DNA binding palindromic motifs for the binding of MoIsw2 to *M. oryzae* DNA sequences.

As mentioned in the introduction, Isw2 proteins are known to preferentially bind DNA at intergenic regions where transposable elements (TEs) are commonly located (Whitehouse et al. 2007) with staggered palindromic motif target sites (Linheiro and Bergman 2008). TEs are also mainly located intergenic in *M. oryzae* in previous unmapped DNA (Chadha and Sharma 2014; Bao et al. 2017) and appear to affect secreted protein expression important for pathogenesis differently in different *M. oryzae* strains (Bao et al. 2017).

Our new data showed hits mainly for intergenic sequences (**Supplemental Data 1**) where the palindromic retrotransposon sequences are preferentially located (Linheiro and Bergman 2008). For these reasons, we looked for palindromic motifs in the ChIP-seq sequences interacting with MoIsw2-GFP. For

this analysis we used the MEME website and as input all sequences (peaks) with the ChIP-seq sequences. In addition, we also searched the ChIP-seq sequences for previously identified RT sequences (Bao et al. 2017).

Three palindromic motifs were found to be common (**Supplemental Data 2**) with 47, 196 (**Fig. 2F)**, and 32 occurrences for motifs 1, 2 and 3 respectively, located at 267 DNA locations. The large majority of these locations are intergenic and only a few ChIP-seq sequences had more than one motif hit. We investigated in detail the motif with 196 hits and the majority of these hits were indeed intergenic (113 intergenic locations), while the rest (63) were in the promoter region of a gene. Using a TOMTOM search at the MEME website, we found that the most common palindromic motif 2 is similar to a known human Myb-binding protein containing a DNA binding motif (**Fig. S4, Supplemental Data 3**).

MoIsw2 DNA binding and its influence on close-by avirulence gene expression.

Transposable elements interacting with MoIsw2 may play a direct role in a pathogen-plant arms race if they affect the expression of the nearby avirulence genes (Chadha and Sharma 2014; Bao et al. 2017) through targeted nucleosome condensation (Bourras et al. 2016; Fijarczyk et al. 2022; Feurtey et al. 2023). Avirulence genes are often effectors the pathogen needs to efficiently cause disease and parasitize the host, but different cultivars of the host acquire resistance against these proteins naturally or through human exploitation in plant breeding

303 programs to develop disease-resistant plant varieties (Jones and Dangl 2006). For
304 these reasons, avirulence genes should preferably have become placed adjacent to
305 the MoIsw2 binding site through evolution, and their expression should be
306 affected differently depending on their closeness to the MoIsw2 binding site.

307 We first made a list of all known avirulence genes noted for *M. oryzae* at
308 NCBI (**Table 1, Supplemental data 9**) to test the above. There are 16 avirulence
309 genes of different types and in addition, the avirulence gene cluster of 12 more
310 genes for a cytochalasan-type compound biosynthesis (Collemare et al. 2008;
311 Song et al. 2015). We then made an RNAseq of the background strain *Ku80* and
312 compared it with the *MoISW2* mutant which also could be compared with the
313 downloaded data. The cytochalasan cluster is specifically activated at early hours
314 post-infection (HPI) during penetration and produces a secondary metabolite
315 recognized by the *R* gene *Pi33* in resistant rice cultivars (Collemare et al. 2008).
316 Two other avirulence genes, Avr-PWL1 and Avr-PWL2 (Dioh et al. 2000),
317 together with the previous, make 18 classic avirulence-type genes, excluding the
318 cytochalasan gene cluster genes (**Table 1**). Most of the genes in the cytochalasan
319 cluster are very closely positioned to MoIsw2 palindromic DNA binding motif
320 sites, and several are differently expressed in strains Guy11 and 98-06 (**Table 1**),
321 which might lead to the production of different final metabolites from the
322 cytochalasan gene cluster even if the different metabolites function as virulence
323 factors.

Six other avirulence genes are not expressed in either strain (**Table 1**). Of these 6 genes, half of the genes are close to the MoIsw2 binding site, and 3 are further away in Guy11. Two avirulence genes (MGG_17614 and MGG_15611) are in supercontigs with unknown gene order in our data, so it is unsure how far they are from a MoIsw2 binding site.

TE position and MoIsw2 DNA binding

We searched the short MoISW2 ChIPseq sequences data for described TEs sequences (Bao et al. 2017) and found described TEs in 92.2 per cent of sequences while the genome outside these ChIPseq sequences is almost devoid of TEs (**Supplemental data 5**). We mapped the MoIsw2 binding sites to the genome as well as the position of all found transposable elements (TEs) (**Fig. 3**). The positioning of the MoIsw2 binding sites and the palindromic motifs we found are close to retrotransposons and the differential regulation. The found expression variation can indicate that MoIsw2-specific targeting is instrumental for stabilizing avirulence gene expression. These data and analyses with additional references are available in supplemental data files (**Supplemental data 4 and 5**). In conclusion, MoIsw2 and RT activities could together be instrumental in creating variation in gene expression profiles between fungal strains.

346 **MoIsw2 regulates the genes closest to the MoIsw2 motif sites in the DNA**

347

348 We next compared the RNAseq for the *Δmoisw2* strain and the background *Ku80*
349 strain for overall gene regulations (**Fig. 4A-B**). There was a general upregulation
350 of the genes closest to the MoIsw2 binding sites in the *ΔMoisw2* mutant (**Fig. 4A**).
351 For these genes, the *ΔMoisw2*/*Ku80* expression ratio is lower when the MoIsw2
352 is predicted to bind directly in the promoter region than for the closest gene for a
353 predicted intergenic binding of MoIsw2. On the other hand, if absolute (positive
354 or negative) regulation was considered both types of genes, with MoIsw2 binding
355 in the promoter region or intergenic, had similar absolute regulation indicating
356 that many genes with MoIsw2 binding in their promoter region are repressed in
357 *ΔMoisw2*. This suggests that without MoIsw2 activity, repressors can also get
358 access to the DNA (**Fig. 4B**). These observations support MoIsw2 as an Isw2
359 protein that creates a local nucleosome condensation at specific nucleosomes
360 (Donovan et al. 2021) increasing genes' either transcriptions or repressions at
361 slightly further distances from the DNA binding sites.

362

363 **Overall functional classification of differentially expressed genes in the**
364 **RNA-seq data**

365

366 In *ΔMoisw2* grown on MM-medium, 339 genes were significantly
367 upregulated relative to the background *Ku80*. The two largest significantly

368 overrepresented gene categories were secondary metabolism and DNA-
369 binding, while most other categories are related to DNA synthesis, DNA-
370 linked activities and other growth-related processes (anabolism) (**Fig. 4C**).
371 These are the genes MoIsw2 likely negatively regulates in the background
372 *Ku80*. Most downregulated genes in the *ΔMoisw2* are genes involved in
373 mitochondrial electron transport, other mitochondrial processes,
374 transported compounds and other processes connected with uptake and
375 respiration and oxidative phosphorylation (catabolism) (**Fig. 4E**).
376 In other words, our results indicate that MoIsw2 is involved in
377 regulating the balance between anabolism and catabolism. Between DNA
378 synthesis, which is safest without ATP generation by mitochondrial
379 respiration since that generates Radical Oxygen Species (ROS), and
380 oxidative phosphorylation, which is more effective in generating ATP from
381 the metabolized substrates (Klevecz et al. 2004).
382
383 **The local gene regulations close to the MoIsw2 palindromic DNA binding**
384 **sites fit the Isw2-specific targeted DNA binding model.**
385
386 DNA is wrapped around and slides around nucleosomes of similar sizes, with a
387 constant overall Nucleosome Repeat Length (NRL) (van Holde 1989; Cutter and
388 Hayes 2015; Donovan et al. 2021; Willcockson et al. 2021) and NRLs sizes vary
389 slightly depending on the organism, cell type and cell status (van Holde 1989).

To further investigate local regulation around at or close to the binding sites with the found palindromic motif, we investigated our RNAseq data and ordered the MGG-codes for the genes in the order of the genes on the chromosomes (Chromosome order downloaded from BROAD).

Dynamic changes due to chromosome packing affected by MoIsw2 should result in the same regulatory landscape in ween in our experiment and the downloaded data. Since MoIsw2 activity depends on respiratory catabolism activity (nutrient availability in the niche) as mentioned above, the greatest variation in expression between experiments should be for genes positioned close to the MoIsw2 binding sites in the DNA. The change of the measured gene expression responses in our RNAsec data and compared expression responses (positive and negative) in Ku80 (background) strain with the *ΔMoisw2* mutant strain (DelR). We could then test if the variation in expression responses (positive and negative) (VarR) in the downloaded data from 55 RNAsec datasets from several labs shows expression variations at similar positions in the data as were affected by the deletion. We found that the two gene expression measurements were Log-Log correlated (P=5.3E-196) and that the response slope of the correlation was 0.56 with VarR on the x-axis (**Fig. S5, Supplemental Data 11**).

We further calculated the gene distance between each gene and the closest MoIsw2 binding site (**Supplemental Data 10**) and plotted that together with plots of the gene expression change from our experiment (DelR) and the variation in the downloaded data (VarR). In the plot (**Fig. 5**), we also included the positions

of the avirulence genes (rings). From these comparisons, one can see that gene regulatory responses along the genome are dependent on MoIsw2 and its binding to DNA. Further, we can identify regions along the DNA with high variation in gene regulation between experiments close (less than 16 genes from the closest motif) to MoIsw2 binding motifs (**Fig. 5** Regions (A-U)) and regions with less variation further away (17-to about 500 genes) from the MoIsw2 binding motifs (**Fig. 5** Regions (1-15)). In **Figure 5** we have marked the positions of the Avir genes as well.

For typical housekeeping genes like the genes encoding ribosomal proteins (Zhang, Zhang, Liu, et al. 2019), their expression depends on the overall rate of translation and should be quite constant between experiments. These genes are mainly found further away from the MoIsw2 binding sites and TEs confirming that the ribosomal proteins are in regions with more stable expression (**Fig. 6A**).

On the other hand, genes that are important for interaction with the environment as the secreted proteins with identified domains (SP) and smaller other secreted proteins (OSP) (Bao et al. 2017) are positioned in the more variable genomic regions closer to the MoIsw2 binding motifs (**Fig. 6B** and **6C, Supplemental Data 6-7**)

Other genes that are important in interaction with the environment are secondary metabolites. Instead of searching the literature, we used the AntiSmash web server and submitted the whole DNA sequence from BROAD to get a more extensive list of putative core secondary metabolite genes. We found 64 core

secondary metabolite genes and plotted their positions along the ordered gene positions (**Fig. 7A, Supplemental Data 8**) and found that they are mainly positioned close to MoIw2 binding motif sites.

Epigenetic silencing can if it is persistent from generation to generation result in the silenced genes accumulating deleterious mutations since the genes are never expressed and needed in the ecological niche the organism lives in. We consider genes not expressed in any of the downloaded RNAsec datasets as potential pseudogenes (PP). Since the misuse of the pseudogene term does not make sense, we follow the nomenclature suggested (Cheetham, Faulkner, and Dinger 2020) and only use the term pseudogene alone for sequences that look like genes and are not expressed at all under natural conditions. Consequently, due to limited knowledge of most microorganisms' natural lifecycles, it is difficult to definitively classify a gene as a vestigial gene or a pseudogene. However, if a gene is rarely expressed under natural evolutionary relevant circumstances and accumulates mutations over time rendering it non-functional, it may eventually become a pseudogene. Several genes close to the *MoISW2* binding sites were not expressed at all in any of the 54 downloaded RNAseq datasets (**Fig. 6B** and **Supplementary Data 4)** indicating that these genes could be or become vestigial genes or pseudogenes without biological roles, thus we call them potential pseudogenes following the definition for the pseudogene concept recently suggested (Cheetham et al. 2020). Our observation that these genes are or have become potential pseudogenes during evolution is exciting since some of these

genes close to the MoIsw2 binding sites are annotated as avirulence effector genes (**see Table 1**).

DNA binding genes

Since 65 genes were classified as DNA-binding and were among the enriched genes upregulated in *ΔMoisw2* (**Fig. 3C, Supplemental Data 13**) these could be conventional TFs, suppressors or other DNA binding genes needed when interacting with the biotic and abiotic environment potentially of high importance during pathogenesis.

The 12 DNA-binding genes most suppressed by MoIsw2 activity are mainly involved in DNA repair (**Table 2**) needed for DNA synthesis and growth. Among the most regulated genes were two TFs and several helicases as well as other genes needed for DNA repair during and after DNA synthesis. A fungal-specific gene involved in (sexual) sporulation is also in this list of 12 DNA-binding genes most suppressed by the MoIsw2 activity.

Functional classification of genes potentially affected by the MoIw2 activity

A. Genes at the MoIsw2 binding sites in DNA sequences

We have above shown that genes under *MoISW2* control that are more expressed in the background *Ku80* strain compared to the *ΔMoisw2* strain are enriched for gene classes associated with secondary metabolism as well as biomass growth

(anabolism) while the genes that are downregulated in the mutant are connected to aerobic metabolism and stress (**Fig. 3C**).

Using the *MoISW2* ChIP-seq data, we investigated the FunCat classification of all genes adjacent to or in ChIP sequence hits to find out what types of genes are overrepresented and which are depleted. First, we removed double ChIP peak sequence hits close to the same gene so as not to count the same gene twice. We then investigated the list of genes that are closest to the found MoIsw2 binding sites. These genes should be targeted by MoIsw2 and might be under positive or negative control from MoIsw2. According to the previous analysis, they should not belong to growth (anabolism) but be genes active when oxygen is consumed, and the substrates oxidized (catabolism) (Klevecz et al. 2004; Machné and Murray 2012). In addition, the binding sequences are located close to avirulence genes and retrotransposons, so their regulation can shift depending on retrotransposon transpositions. Note that since ChIP-seq only shows potential binding to DNA *in vitro,* we cannot say if these genes are up or downregulated; only that a regulation influenced by MoIsw2 is possible.

Genes with ChIP binding hits closest to the MoIsw2 palindromic DNA binding motif site are mainly enriched for genes involved in secondary metabolism and other gene classes important for biotic interactions (**Fig. 7A)**. In contrast, categories of genes for biomass growth and housekeeping (anabolism) are depleted (**Fig. 7B**).

Many other genes within ChIP-seq sequences could be affected. These genes are many more than those closest to the MoIsw2 palindromic DNA motif2 sites. For these (**Fig. 7C**)., we find more gene classes including detoxification and signalling (cyclic nucleotide-binding), disease, and defence, and these are all important gene classes involved in biotic and abiotic interactions with the environments. Depleted are gene classes characteristic for anabolism (biomass growth) (**Fig. 7D**).

Finally, the genes in the ChIP-seq data but not with motif2 hits (not containing the MoIsw2 palindromic DNA binding motif 2 sites) are again genes enriched for secondary genes and again genes involved in abiotic and biotic interactions (**Fig. 7E**). Genes needed for biomass growth are depleted (**Fig. 7F**).

Functional classification of 500 genes showing the highest VarR and DelR values.

As we have seen above (**Fig. 7**) the genes close to MoIisw2 binding motif123 are in general more variable expressed DNA regions between RNAsec plant infection experiments (VarR). These regions number the most TEs and core secondary metabolite genes. To get more information on functional classes regulated we used FungiFun again and did a functional classification of the 500 most variable genes (VarR) in the downloaded data and compared that with the genes most affected by the *MoISW2* deletion (**Fig. 9, Supplemental Data 12**). Few of these

genes are probably directly regulated by MoIsw2 but the access to them for gene regulation should be affected. Furthermore, similarities and differences between VarR and DelR should point to regulations biased for genes important for plant interactions or plate growth respectively.

Genes categories needed to cope with the abiotic and biotic environment are enriched among the 500 with the highest VarR **and** DelR values indicating that both the lab and inside plants' similar gene functions are in principle affected by the MoIsw2 activities (**Fig 9A**). Depleted functional gene classes are growth-related genes (anabolic) and some stress-related genes (**Fig 9B**).

Genes categories needed to cope with the abiotic and biotic environment are again enriched among the VarR 500 most differentially regulated gene classes (**Fig. 9C**). Depleted are again growth-related genes (anabolic) and stress-related gene classes (**Fig. 9D**).

The fungal biomass had recently been shifted from stationary (agar plugs) with the nuclei in various states of growth to a liquid medium for 48h triggering vigorous growth. Thus, variations in the genes affected by the deletion (DelR) are expected in genes for how fast the biomass reacts to the new situation of plenty of nutrients also for genes not affected by MoIsw2 activities. That is probably why unfolded protein response genes are among the enriched genes most affected by the deletion in DelR (**Fig. 9E**), . But in general, the functional gene classes among the most regulated VarR alone and most deletion-affected DelR alone are similar.

The specifically differential regulation during plant infection (VarR-specific genes) are genes that are expected to be genes classes responding in fungal-innate immunity (Ipcho et al. 2016) (reacting to plants in this case) (**Fig. 10A-B**) and are further discussed in the discussion section. The DelR-specific enriched and depleted gene classes (**Fig. 10 C-D**) indicate gene classes important to regulate during fast aerobic growth of hyphal biomass and nutrient uptake from the environment *in vitro*.

Discussion

Deletion effects on phenotypes, and regulation (DelR) compared with variability in regulation between RNAseq experiments (VarR).

When *MoISW2* is deleted, the general growth of the fungus (**Fig. 1**) was negatively affected, as was the sensitivity to SDS and NaCl. Conidiation was completely abolished as was also pathogenicity, and the MoIsw2-GFP fusion accumulates in the nucleus as expected for a nuclear localized protein. The strong effect on infection and the fact that Isw2 proteins are known to affect the regulation of many genes in genomes through local chromosomes around several DNA binding sites (Fazzio et al. 2005) indicates that *MoISW2* could be a "master regulator" for regulating the many fungal defences against the plant defences. This is because these and virulence factors (for example secondary metabolism) are especially upregulated in the biotrophy/necrotrophy transition, and during the necrotrophic stage (Andrew et al.

565 2012; Kou et al. 2019) when membrane effects on the pathogens are especially
566 prominent and the fungus have to deal with plant ROS defences.

567 We found that potential effector genes like avirulence genes, secreted
568 proteins, and core secondary metabolite genes are located in the DNA regions that
569 appear to be under MoIsw2 control. The protein appears to have the role of a
570 master regulator of TF and repressor gene access to genes necessary for the fungus
571 reacting with the biotic and abiotic environment (**Fig. 5, 6, 7A**) since these gene
572 types are in regions of the DNA that are differentially regulated in the *ΔMoisw2*
573 compared to the background K80 (DelR). These regions are also the same regions
574 with the highest variability between experiments in a set of RNAseq data from 55
575 downloaded RNAseq datasets from experiments in planta (**Fig. 5**) (VarR). That
576 is what could be expected for nich determinant genes that are not involved in the
577 basic metabolism.

578 The overall regulation effect of all genes in the two datasets (VarR and
579 DelR) were correlated as they should be if the regulated regions in the two datasets
580 were the same and strain-specific and not experiment-specific and only dependent
581 on the MoIsw2 activity caused organisation of chromatin in the particular strain.
582 Growth inside a plant is stressful for a plant pathogen. The fungus must
583 compete with the plant for all nutrients during the biotrophic stage without
584 revealing its existence and then trigger plant immunity responses that it has
585 to handle in the necrotrophic stage (Andrew et al. 2012; Chowdhury et al. 2017;
586 Rajarammohan 2021). When shifting to the necrotrophic stage the

pathogenic fungus must thus both overcome plant defences and nutrient limitations since when spreading inside the plant, nutrient limitations might occur (Josefsen et al. 2012). In support of a strain-specific "master regulator" function for MoIsw2 regulating responses to environmental conditions, we find that many fungal defence and virulence-related functional gene classes are regulated and positioned in the variably regulated chromosomal regions that appear to be under MoIsw2 activity control (**Fig. 8 and 9**). There is in addition a difference in the regulation of avirulence genes between *M. oryzae* strains and these genes are situated close to the MoIsw2 binding sites in the DNA giving the strain specificity of the MoIsw2 as master regulator further support (**Table 1**).

Regulation of chromatin condensation by nucleosome positioning

MoIsw2 is a true Isw2

Direct interactions with His4 could not be detected by a yeast two-hybrid assay. The yeast Isw1 and Isw2 interactions with His4 are transient (approximately 200 and 80 bindings per minute, respectively) and need a continuous ATP supply (Tsukiyama et al. 1999). Similarly, the interaction in human cells has been measured in vivo using advanced microscopy and spectroscopy techniques and found to be transient (10-150ms)(Erdel et al. 2010; Erdel and Rippe 2011). Thus, our attempts to detect an interaction between MoIsw2 and MoHis4 using the yeast two-hybrid method were in

609 vain. On the other hand, the expression of MoIsw2 and the expression of
610 orthologues to genes in *M. oryzae,* that an Isw2 protein are known to
611 physically interact and form a functional Isw2 protein complex (Donovan et
612 al. 2021), are correlated (**Fig. 2**). That indicates that MoIsw2 is a true Isw2
613 with a conserved Isw2 protein function and it has a conserved order of
614 domains in the protein (**Fig. 1A**)
615
616 **Regulation of MoIsw2 activity and regulation by *MoISW2* expression**
617 Isw1 translocates nucleosomes away from other nucleosomes, while Isw2
618 translocates towards the centre of DNA pieces and other nucleosomes *in*
619 *vitro,* with the nucleosomes bound to relatively short DNA pieces
620 (Kagalwala et al. 2004; Zofall et al. 2004). It does the same *in vivo* where it
621 was found that Isw2 is mainly involved in the targeted regulation of DNA
622 access close to the Isw2 DNA binding site (Fazzio et al. 2005), as we also
623 find (**Fig. 4, Table 1**).
624 The Isw2 activity is ATP dependent (Whitehouse et al. 2007; Hota and
625 Bartholomew 2011; Dang et al. 2014). Thus the regulation of genes adjacent
626 to the DNA-binding site is likely to be highly dependent on ATP
627 availability and competition for ATP in the cytoplasm-nucleus
628 compartment. ATP generation from fermentation is much faster but less
629 efficient than from oxidative phosphorylation when fast fermentation is
630 possible. In yeast, growth is characterized by DNA replication, mainly

without mitochondrial oxidative activity (fast aerobic glycolysis), most probably to protect DNA from mutations (Klevecz et al. 2004). In *M. oryzae,* MoIsw2 could thus be an ATP-regulated switch (Machné and Murray 2012) between fast aerobic glycolysis accompanied by DNA-synthesis growth with quality control, and slower but more efficient oxidative phosphorylation growth with high ATP yield, active oxidative defences, and interaction with the abiotic and biotic environment that makes up the *M. oryzae* ecological niche. In support of this, we found that genes upregulated in the *ΔMoisw2* mutant and thus repressed by MoIsw2 under other more ATP-limited aerobic growth conditions are involved in fast growth and DNA synthesis, DNA quality control, while downregulated genes in the mutant were those involved in oxidative phosphorylation, stress management, and secondary metabolite biosynthesis (**Fig. 3EF** and **Table 2**). As also expected from the known function of Isw2, the genes closest to the two central immobilized nucleosomes at the MoIsw2 DNA-binding sites are downregulated in the background *Ku80* (Donovan et al. 2021), and when *MoISW2* is deleted, these genes are upregulated (**Fig. 3A**).

Regulation by MoIsw2 is dependent on distance from the MoIsw2 DNA binding sites.

Gene regulation affected in the *ΔMoisw2* mutant strain compared to the background Ku80 strain (DelR) as well as the variation between RNAseq

653 experiments (VarR) are dependent on the distance from the MoIsw2 DNA
654 binding motif sites (**Fig. 5**). That agrees with that regulation is a
655 consequence of the MoIsw2 positioning of the closest nucleosomes giving
656 more sliding space to surrounding nucleosomes (Donovan et al. 2021) and
657 consequently increased DNA access. Genes affected by the MoIsw2 activities
658 and being physically close to the palindromic binding sites in the DNA are
659 for example genes for secreted protein while core secondary metabolites
660 while typical housekeeping genes like genes encoding ribosomal proteins
661 are much further away (**Fig. 6**). In support of this we found that the 500
662 most regulated genes (High VarR and/or DelR) with most variable gene
663 expression were significantly enriched for functional gene classes needed
664 to react to the biotic and abiotic environment and depleted for typical
665 housekeeping genes (**Fig. 9**). Interestingly, and in line with this
666 interpretation, the 500 genes specifically upregulated in VarR (during plant
667 pathogenesis) and in DelR (growth in vitro) are genes that reflect the two
668 different biotic/abiotic environments for the fungus. The functional gene
669 classes specially enriched in VarR (especially the ones in red text) are those
670 that are expected for fungal innate immunity (Ipcho et al. 2016) and
671 protection against plant innate immunity like the removal of fungal cell
672 wall derived aminosaccharides (chitin oligomers) that triggers plant
673 immunity (Nürnberger et al. 2004) (**Fig. 10A**).
674

Conserved and variable DNA

Our observations suggest that the *M. oryzae* genome is organized into regions with constant expression and variable expression depending on the environment. The regions with variable expression are close to MoIsw2 DNA binding sites and contain genes important for the interaction with the environment (during biotic and abiotic stresses) while regions with less variable expression contain housekeeping genes. Such a division of the fungal genome into regions of housekeeping genes and niche-determinant faster-evolving genes is consistent with previous findings in the relatively closely related *Fusarium graminearu*m (Zhao et al. 2014) but also in *V. dahliae* (Faino et al. 2016).

Palindromic sequences are characteristic of retrotransposons that are mainly positioned close to stress-related genes and avirulence genes in the genomes of fungal plant pathogens. Fungal avirulence genes are plant-pathogen effectors that trigger different plant immunity responses depending on plant variety and the basis for plant cultivar-specific resistance to specific pathogen strains (the gene-for-gene relationship) (Bourras et al. 2016) and we find them close to MoIsw2 binding motifs (**Table 1, Fig. 5**). The *MoISW2* DNA binding sequences (the ChIPseq sequences) also contained palindromic DNA motifs characteristic of the identified TEs (Bao et al. 2017) (**Fig. 4**). A palindromic DNA motif gives genetic instability to the genome at the site of the motif (Ganapathiraju et al.

2020; Svetec Miklenić and Svetec 2021). Stress, virulence, and stress-related genes are in *V. dahliae* (Faino et al. 2016) as well as in *M. oryzae,* are also linked to transposable elements (Yoshida et al. 2016) and we see this in our study as well (**Fig. 6, 7A, 8-10**).

Different mutation rates or mutation bias of genes have recently been described as a new concept for the plant *Arabidopsis thaliana* (Monroe et al. 2022). Genes with higher mutation rates are involved in biotic and abiotic interactions. The gene found with the highest mutation rate was a gene responding to chitin, which is present in symbiotic (pathogenic and nonpathogenic) fungi and insects (Monroe et al. 2022). Transposable element activity seems important in fungal speciation (Faino et al. 2016) and tends to accumulate in genomes and expand the genome with repetitive sequences (Fijarczyk et al. 2022; Feurtey et al. 2023) unless there is some evolutionary constraint against such expansion (Kremer et al. 2020; Fijarczyk et al. 2022). Phosphorous availability is a possible constraint (Ågren et al. 2012) since a considerable amount of the cell phosphorous, especially, is bound up in DNA and not available for other purposes (Berdalet et al. 1994). Fungal plant parasites can get phosphorous directly from their plant hosts by degrading the plant tissue and are not so restricted by limited resources in the soil (Ågren et al. 2012). Thus plant parasitic fungi should be expected to have more retrotransposons to adapt better to plant resistance and thus have relatively large genomes. That is precisely what they have (Fijarczyk et al. 2022; Feurtey et al. 2023). Endophytic fungi that have to coexist with their host in their

719 life cycle, and thus have to compete with the host for phosphorous, should, in
720 consequence, have smaller genomes, as they also seem to have (Fijarczyk et al.
721 2022).

722 Our results show changes in occurrence and regulation of the
723 avirulence genes between two *M. oryzae* strains with different
724 pathogenicity to different rice cultivars (**Table 1**). In addition, we did not
725 detect any expression for some putative avirulence genes close to the
726 MoIsw2 DNA binding sites, suggesting that those genes may be potential
727 pseudogenes in these strains. That might indicate a retrotransposon-aided
728 genetic evolution of inherited epigenetic changes to regulation in reactions
729 to the environment (resistance of the plant cultivar) as has been indicated
730 for *V. dahliae* (Faino et al. 2016). Such regulation can become genetically
731 fixed, first through loss of possible regulation (making downregulated
732 genes into pseudogenes), and much later complete gene loss or change of
733 the potential pseudogenes so they cannot be easily recognized as genes, is
734 a mechanism that could result in a "biased" faster evolution (Chadha and
735 Sharma 2014). Most of the potential pseudogenes (not expressed under any
736 conditions reported in this paper) were close to the MoIsw2 DNA binding
737 sites with palindromic motifs supporting this hypothesis for a mechanism
738 involving MoIsw2 activity in creating pseudogenes and complete removal
739 of genes by making them unrecognizable as genes through mutations. A
740 prerequisite for this to happen is that the ecological niche does not change

as fast as it can for a plant pathogen because of efforts of resistance breeding of susceptible plant cultivars. These efforts can then reactivate the silenced genes by TE repositioning to chromosome areas with changed MoIsw2 activity.

Our results further indicate that *MoISW2* regulates a switch between fast glycolytic growth with fast DNA synthesis and slower but nutrient-efficient aerobic stress-characterized growth with less DNA synthesis, coping with abiotic and biotic stresses or, in other words, niche fitness. The loss of *ISW2* function in a unicellular Eukaryote or the early stages of fungal growth from a spore should make the fungus unfit for survival in a natural environment and become more dependent on aerobic fermentation for ATP synthesis that is not substrate efficient although generates ATP at a very high rate although inefficient (Pfeiffer and Morley 2014; Desousa et al. 2023). However, a limitation for eukaryotic cells to only aerobic fermentation generally leads to uncontrolled cell growth and oncogenesis in a long-lived multicellular organism (Desousa et al. 2023), as ATP and fermentable nutrients can be received from surrounding cells and other tissues through the blood circulation. Thus, mutations of the genes *SMARKA2* or *SMARKA4* that encode Brm and Brg1 proteins that are orthologues of fungal Swi2/Snf2 can cause cancer (Reisman et al. 2009; Mittal and Roberts 2020; Li et al. 2021).

On the other hand, a general shift to aerobic glycolysis and a fast upregulation (within a few hours) of innate immunity-related genes and their ATP-dependent translation is associated with tissue inflammation. Such fast de-novo protein synthesis is characteristic of fast defence against microbes needing rapid translational responses and has been shown for *Fusarium graminearum* but is general for eukaryotes (Ipcho et al. 2016). Such fast upregulated plant innate immune responses can be inhibited by fungal-derived immune system inhibitors acting on translation like trichothecenes the fungus (Toyotome and Kamei 2021), most likely to attenuate immune responses in the plants it infects. In line with a fungal innate immunity scenario (Ipcho et al. 2016), genes involved in RNA synthesis and RNA processing were found to be upregulated in the *ΔMoisw2* mutant (**Fig. 3C**).

Is retrotransposon shifting *MoISW2* binding creating and directing the mutation bias by adapting the fungus to new challenges?

MoISW2 is likely an important player in a mechanism aiding both mutation bias and adaptation to new circumstances whose combined activities lead to two-speed evolution of the fungal genome (Faino et al. 2016) a slow random evolution and a fast more directed by adaptations. The faster speed evolution can be named natural adaptation-directed fast evolution (NADFE), a new concept that is similar to artificial adaptation-directed fast evolution that can be performed in a laboratory (Packer and Liu 2015). The suggested mechanism is

784 the following: As transposon DNA containing MoIsw2 palindromic DNA binding
785 sites seems necessary for MoIsw2 activity, stress-activated transposon activity,
786 known for creating genomic instability, can together with the MoIsw2 activity
787 create a new adaptive regulatory landscape (Chadha and Sharma 2014) that can
788 be stabilized relatively quickly and lead to mutation bias (Monroe et al. 2022). In
789 addition, the Isw2 stabilized expression landscape further stabilized by later
790 mutations could be the mechanism sought after for a Lamarckian-Darwinian
791 synthesis. This mechanism can explain the fast evolution of new traits requiring
792 many combined mutations that cannot be reconciled within Darwinian strict
793 random evolution creating variation together with sexual recombination and
794 natural selection to cause both the observed direction and the needed speed of
795 evolution of specific traits when new niches become available, or there are drastic
796 niche changes (Bard 2011). The chance of multiple mutations that only together
797 can become positive is theoretically much more likely to happen with NADFE
798 first creating a mutation bias (Monroe et al. 2022).
799
800 **Perspectives for Future Research**
801 *Evolution of the plant-pathogen interaction:* The effect of exposing *M.*
802 *oryzae* strains to different MoIsw2 activities and retrotransposon activities
803 on the rate of genetic adaptation to a shift in rice cultivar is a possible future
804 topic that could be exploited to understand how the pathogen adapts to
805 different resistant cultivars and break plant resistance.

Agrochemicals: Searching for potential agrochemicals to manipulate MoIsw2 activities on His4 and DNA-binding is tempting since *MoISW2* is crucial for plant pathogenicity. Though MoIsw2's close resemblance to mammalian proteins with the same function indicates that such chemicals are likely negatively affecting orthologue proteins in mammals and might be cancerogenic to humans since even small mutations in *ISW2* orthologues in mammals can cause cancer (Reisman et al. 2009; Mittal and Roberts 2020).

Histon4: Finally, we found 2 *MoHIS4* genes with large differences in DNA sequences (gene duplication many generations ago) predicted to encode for identical proteins but differently regulated and it seems like *M. oryzae* needs both genes (**Fig. 2**). This fact is of interest since His4 proteins in nucleosomes is what MoIsw2 is supposed to interact with (Tsukiyama et al. 1999), and *HIS4*s are examples of genes with the highest degree of purifying evolution (Piontkivska et al. 2002). We have thus started new research into the roles and regulation of these two *MoHIS4* genes and how their regulations shift with growth conditions. Their predicted identical amino acid sequences indicate that they are evolutionarily constrained to differ only by synonymous mutations.

Gene expression variability: The most interesting genes for biotic and abiotic interactions are also the genes with the highest variability between experiments (VarR) creating problems when proving the effects gene deletions. The common practice of only using 3 replicates for measuring

effects on genes (like deletions) is probably not enough and we might need to increase the number of replicates to 5 for the gene expression in the wild type. If we do that we can either statistically prove what type of distribution there is and use that or better use non-parametric methods not assuming the distribution. Strict normal or more correctly lognormal distribution (negative expression is not possible!) may also be true mainly for housekeeping genes.

Consequences of MoIsw2 functions that are positive for the fungus's ability to stay pathogenic: 1. The MoIsw2 function will result in adaptive silencing of virulence/avirulence genes without gene loss due to mutations of the actual DNA nucleotides. In other words, virulence genes are not quickly lost from the adapted strains but can be "called upon again" if the available hosts change their resistance in the classical gene-for-gene scenario (Flor 1956). 2. Adaptive silencing of virulence genes is often found close to transposable elements (Menardo et al. 2017) and that will lead to biased fast gene evolution of especially genes involved in biotic interaction (Monroe et al. 2022) and in the gene-for-gene concept and is a possible mechanism behind the speedy appearance of virulent pathogen strains capable of attacking newly developed resistant plant varieties (Palloix et al. 2009; Menardo et al. 2017).

Materials and Methods

Fungal strains and media

Magnaporthe oryzae B. Couch anamorph of the teleomorph *Pyricularia oryzae* Cavara was used for this research. As background strain, we used Ku80 (generated from the WT strain 70-15) to minimize random integration events when transformed (Villalba et al. 2008). The susceptible Indica rice (cv. CO-39) and barley (cv. Golden Promise) used for the fungal pathogenicity tests were from the seed bank of our laboratory. For both ChIP-seq and RNAseq, the strains used were grown and harvested similarly.

Knockouts, complementations, and verifications

The *MoISW2* is a *MYB* gene and *MYB* gene deletion vectors were constructed in the plasmid pBS-HYG by inserting 1 kb up- and down-stream fragments of the target gene's coding region as flanking regions of the HPH (hygromycin phosphotransferase) gene (Li et al. 2012). No less than 2 μg of the deletion vector DNA of the target gene was introduced to Ku80 protoplasts, and transformants were selected for hygromycin resistance to perform gene deletion transformations. Southern blotting was conducted to confirm the correct deletion using the digoxigenin (DIG) high prime DNA labelling and detection starter Kit I

872 (11745832910 Roche Germany). The *MYB* gene complementation vectors were
873 constructed by cloning the entire length of the target gene with the native promoter
874 region (about 1.5 kb) to the pCB1532 plasmid. When making the
875 complementation vector, GFP was linked to the C-terminal of the target genes to
876 study the sub-cellar localization of Myb proteins. The constructed vector DNA
877 was introduced into the mutation protoplast for gene complementation, and
878 resulting transformants were screened using 50 μg/ml chlorimuron-ethyl to select
879 successful complementation strains. Detailed fungal protoplast preparation and
880 transformation methods have been described previously (Li et al. 2012). All
881 primers needed for the knockout and complementation are listed (**Table S1**). The
882 sub-cellar localization of Myb proteins was observed by confocal microscopy
883 (Nikon A1). GFP and RFP excitation wavelengths were 488 nm and 561 nm,
884 respectively.
885
886 **Colony growth and infection phenotype measurements**
887 Vegetative growth was tested by measuring the colony diameter after ten days of
888 growth in 9 cm Petri dishes at 25℃ under 12h-to-12h light and dark periods.
889 Conidia production was evaluated by flooding the 12-day-old colony with double
890 distilled water, filtering out the mycelia with gauze, and counting the conidia
891 using a hemacytometer. The conidiophore induction assay was performed by
892 excising one thin agar block from the fungal colony and then incubating it in a
893 sealed chamber for 24 h with constant light (Li, Yan, et al. 2010). Mycelia

appressoria was induced by placing a suspension of mycelial fragments on a hydrophobic surface in a humid environment at 25℃ for 24h. The pathogenicity assay on rice was performed by spraying 5 ml conidial suspension (5×10^4 spores/ml) on 15-day-old plants (Y. Li et al. 2019). The inoculated plants were kept in a sealed chamber with a 90% relative humidity at 25℃ for 24 h before the inoculated plants were removed from the chamber to allow disease symptoms to develop for 4-5 days. The pathogenicity assay on excised barley and rice leaves was performed by cutting a small block from the agar culture of the fungus and placing it on excised leaves for five days in a moist chamber for disease development (Li, Liang, et al. 2010). Sexual reproduction was tested by crossing the tested strain with the sexually compatible strain TH3 on OM plates and then incubating at 19℃ for 30 days with continuous light. The perithecia and clavate asci were photographed in a microscope equipped with a camera (OLYMPUS BX51).

Biomass production for ChIPseq and RNAseq

For ChIP-seq, the complemented strain, MoIsw2-GFP and the strain Ku80 were used, and for RNAseq *ΔMoisw2* and *Ku80* were used. The strains were grown on Complete medium 2 (CM2) all are quantities L^{-}: 20X Mineral salts solution 50mL, 1000X Trace element solution 1mL, 1000X vitamin solution 1mL, D-glucose 10g, peptone 2g, casamino acid 1g, yeast extract 1g, pH 6.5. For agar medium add 15g

agar. Supplemented with 20×Mineral salts solution (per 1000mL): NaNO3 120g，KCl 10.4g， MgSO4 7H2O 10.4g， KH2PO4 30.4g and with 1000X Vitamin solution (per 100mL): Biotin 0.01g, Pyridoxin 0.01g, Thiamine 0.01g, Riboflavin 0.01g, PABA (p-aminobenzoic acid) 0.01g, Nicotinic acid 0.01g and 1000X Trace element (per 100mL): $ZnSO_4$ $7H_2O$ 2.2g, H_3BO_3 1.1g $MnCl_2$ $4H_2O$ 0.5g, $FeSO_4$ $7H_2O$ 0.5g $CoCl_2$ $6H_2O$ 0.17g, $CuSO_4$ $5H_2O$, Na_2MoO_4 $5H_2O$ 0.15g, EDTA 4Na 5g. The plates were incubated for 4-5 days at 28°C with alternating light-dark cycles (12/12). Mycelial disks (15-20) were punched out at the colony's edge using a 5 mm diameter cork puncher. The disks were transferred to 100 ml CM2 liquid medium and shake cultured for another 48h (160 RPM, Constant temperature culture oscillator, ZHWY-2102C, Shanghai Zhicheng Analytical Instrument Manufacturing Co., Ltd.). The obtained biomass was filtered using Miracloth, frozen in liquid nitrogen, and sent on dry ice to the company performing the RNAseq.

ChIP-seq and RNA-seq

Both these techniques were carried out by the company Wuhan IGENEBOOK Biotechnology Co., Ltd, China, according to their method descriptions **(Supplemental Company Methods file**). The last steps about finding motifs and enriched gene classes were carried out differently and are described in this paper. These steps not used are marked in the two Supplementary method files.

936

937 **Method for calculating VarR and DelR in the RNAseq data.**

938 We calculated the variability in gene expression for each gene for all the
939 downloaded experimental datasets in the following way. First, we checked that
940 the quality of the data was ok. We have previously found for our own
941 transcriptomic data that a dataset is ok if expressions of genes are rank-ordered
942 then the log log expression of log expression level against the log-rank order
943 should be a smooth downward slightly curved line without big gaps. Also, to be
944 able to compare different sets of data from different experiments the total
945 expression of all genes summed should be similar for all datasets. Next, we
946 calculated the maximum variation between experiments in the following way.
947 The maximum expression value and the minimum expression value for each
948 gene across the 55 transcriptomes were found. Next, we calculated the average
949 expression for the same data. Finally, we calculated the ratio of maximum
950 expression minus minimum expression divided by the average expression to
951 arrive at the variation in expression across all experiments for each gene (VarR).
952 In this way any regulation up or down is treated in the same way as access for
953 TFs and repressors to the DNA should be treated equally. Finally comes the
954 problem that some genes had expression values lower than the threshold for
955 detecting them at all (0-values). For these data, we assumed that the expression
956 where at the threshold value instead of 0 and set the expression to that value. In

that way, we could include that data without overestimating the VarR for that gene.

The effect of the *MoISW2* mutation (DelR) was estimated in the following way to make it comparable with VarR: For each gene, we calculated the 2Log ratio of the expression in the mutant divided by the expression in the background. That results in both negative and positive values. Then these values were squared to arrive at only positive values in a similar way as is done with the least square method for curve fitting to arrive at a better estimate of the deviation from the slope. There were very few genes with no detectable expression so no need for handling zero values more than excluding them.

Note that in this paper, we focus on the expression variation of all genes along the chromosomes. Thus, it is the overall pattern that is important and not the values for a single gene. In none of the methods above we used any method for excluding a gene from the analysis based on an arbitrary threshold of 2 times up or down or any other statistically significant threshold for genes. In consequence, the calculated values for a single gene cannot and should not be relied upon even if a general increased regulation of many adjacent genes has reliability.

Additional software and add-ins for MS Excel

Addins for MS Excel: The **Fisher Exact** add-in for MS Excel was downloaded from http://www.obertfamily.com/software/fisherexact.html. The **Excel solver** was used to fit non-standard equations to data. The Solver is usually part of MS Excel but must be activated in settings.

Freeware: We used the freeware PAST A simple-to-use but powerful freeware program is available from the University of Oslo, Natural History Museum **https://www.nhm.uio.no/english/research/infrastructure/past/** (Hammer et al. 2001) version 4.08 (released November 2021). We mainly used the software for Reduced Major Axis (RMA) regression analysis to handle errors in both the x and y variables. For simplicity, the data was handled and entered in MS Excel and then copy-pasted into PAST for analysis. The resulting plots were exported from PAST as SVG vector graphic files to be later translated into other vector graphic file formats.

Websites used for analyses and getting necessary additional data

NCBI: **https://www.ncbi.nlm.nih.gov/** (sequence downloads, blasts, annotations including domain annotations)

BROAD: **ftp://ftp.broadinstitute.org** (download of gene order on supercontigs for the Guy11 strain, 1000 upstream DNA sequences for use in MEME)

MEME: https://meme-suite.org/meme/ (use of MEME and FIMO). (Bailey et al. 2015).

See the supplemental file for MEME settings and complete results (Supplemental Data 2). MEME motif 2 was the one with the most hits and was investigated in detail. This motif2 was used for TOMTOM by using the direct link to TOMTOM using the link from the MEME result, for results see the supplemental file (Supplemental Data 3).

FungiFun2 https://elbe.hki-jena.de/fungifun/fungifun.php (Priebe et al. 2015)

Species**:** *Magnaporthe grisea* 70-15 (synonym for *M. oryzae* 70-15).

Classification ontology: FunCat (contains more relevant categories for fungal plant pathogens than Kegg or GO)

Input IDs: For *M. oryzae* 70-15 the MGG_ codes has to be used.

Advanced settings used**:** Significance level; 0.05. Significance test; Fisher's exact test. Test for; Enrichment or Depletion. Adjustment method; No adjustment. Annotation type, Select also indirectly annotated categories.

These settings using "No adjustment" were used since the purpose was not to get super reliable enriched or depleted categories but to compare several FungiFun runs with different Gene ID sets.

antiSMASH

The complete DNA sequence of *M. oryzae* 70-15 was downloaded from BROAD. That was then submitted to antiSMASH (Blin et al. 2021) fungal version **https://fungismash.secondarymetabolites.org/#!/start** and run with default parameter settings to find the core genes predicted to be involved in producing secondary metabolites.

Acknowledgements

This work was supported by grants from the Fujian Provincial Science and Technology Key Project (2022NZ030014) Fujian Natural Science Foundation project (2022J01125).

1029 References

1030 Ågren GI, Wetterstedt JÅM, Billberger MFK. 2012. Nutrient limitation on terrestrial plant
1031 growth – modeling the interaction between nitrogen and phosphorus. *New Phytologist*
1032 194:953–960.

1033 Allan AC, Espley RV. 2018. MYBs Drive Novel Consumer Traits in Fruits and Vegetables.
1034 *Trends in Plant Science* 23:693–705.

1035 Ambawat S, Sharma P, Yadav NR, Yadav RC. 2013. MYB Transcription Factor Genes as
1036 Regulators for Plant Responses: An Overview. *Physiol Mol Biol Plants* 19:307–321.

1037 Andrew M, Barua R, Short SM, Kohn LM. 2012. Evidence for a Common Toolbox Based on
1038 Necrotrophy in a Fungal Lineage Spanning Necrotrophs, Biotrophs, Endophytes, Host
1039 Generalists and Specialists.Stajich JE, editor. *PLoS ONE* 7:e29943.

1040 Bailey TL, Johnson J, Grant CE, Noble WS. 2015. The MEME Suite. *Nucleic Acids Res*
1041 43:W39–W49.

1042 Baldoni E, Genga A, Cominelli E. 2015. Plant MYB Transcription Factors: Their Role in
1043 Drought Response Mechanisms. *Int. J. Mol. Sci.*:41.

1044 Bao J, Chen M, Zhong Z, Tang W, Lin L, Zhang X, Jiang H, Zhang D, Miao C, Tang H, et al.
1045 2017. PacBio Sequencing Reveals Transposable Elements as a Key Contributor to
1046 Genomic Plasticity and Virulence Variation in Magnaporthe oryzae. *Molecular Plant*
1047 10:1465–1468.

1048 Bard JB. 2011. The next evolutionary synthesis: from Lamarck and Darwin to genomic
1049 variation and systems biology. *Cell Commun Signal* 9:30.

1050 Berdalet E, Latasa M, Estrada M. 1994. Effects of nitrogen and phosphorus starvation on
1051 nucleic acid and protein content of *Heterocapsa* sp. *Journal of Plankton Research*
1052 16:303–316.

1053 Blin K, Shaw S, Kloosterman AM, Charlop-Powers Z, van Wezel GP, Medema MH, Weber
1054 T. 2021. antiSMASH 6.0: improving cluster detection and comparison capabilities.
1055 *Nucleic Acids Research* 49:W29–W35.

1056 Bourras S, McNally KE, Müller MC, Wicker T, Keller B. 2016. Avirulence Genes in Cereal
1057 Powdery Mildews: The Gene-for-Gene Hypothesis 2.0. *Front. Plant Sci.* [Internet] 7.
1058 Available from: http://journal.frontiersin.org/article/10.3389/fpls.2016.00241

1059 Cao Y, Chen J, Xie X, Liu S, Jiang Y, Pei M, Wu Q, Qi P, Du L, Peng B, et al. 2022.
1060 Characterization of two infection-induced transcription factors of *Magnaporthe oryzae*
1061 reveals their roles in regulating early infection and effector expression. *Molecular*
1062 *Plant Pathology* 23:1200–1213.

1063 Cao Y, Li K, Li Y, Zhao X, Wang L. 2020. MYB Transcription Factors as Regulators of
1064 Secondary Metabolism in Plants. *Biology* 9:61.

1065 Chadha S, Sharma M. 2014. Transposable Elements as Stress Adaptive Capacitors Induce
1066 Genomic Instability in Fungal Pathogen Magnaporthe oryzae.Han K-H, editor. *PLoS*
1067 *ONE* 9:e94415.

1068 Cheetham SW, Faulkner GJ, Dinger ME. 2020. Overcoming challenges and dogmas to
1069 understand the functions of pseudogenes. *Nat Rev Genet* 21:191–201.

1070 Chowdhury S, Basu A, Kundu S. 2017. Biotrophy-necrotrophy switch in pathogen evoke
1071 differential response in resistant and susceptible sesame involving multiple signaling
1072 pathways at different phases. *Sci Rep* 7:17251.

1073 Collemare J, Pianfetti M, Houlle A, Morin D, Camborde L, Gagey M, Barbisan C, Fudal I,
1074 Lebrun M, Böhnert HU. 2008. *Magnaporthe grisea* avirulence gene *ACE1* belongs to
1075 an infection-specific gene cluster involved in secondary metabolism. *New Phytologist*
1076 179:196–208.

1077 Cutter AR, Hayes JJ. 2015. A brief review of nucleosome structure. *FEBS Letters* 589:2914–
1078 2922.

1079 Dang W, Sutphin GL, Dorsey JA, Otte GL, Cao K, Perry RM, Wanat JJ, Saviolaki D,
1080 Murakami CJ, Tsuchiyama S, et al. 2014. Inactivation of Yeast Isw2 Chromatin
1081 Remodeling Enzyme Mimics Longevity Effect of Calorie Restriction via Induction of
1082 Genotoxic Stress Response. *Cell Metabolism* 19:952–966.

1083 Desousa BR, Kim KK, Jones AE, Ball AB, Hsieh WY, Swain P, Morrow DH, Brownstein
1084 AJ, Ferrick DA, Shirihai OS, et al. 2023. Calculation of ATP production rates using
1085 the Seahorse XF Analyzer. *EMBO Reports*:e56380.

1086 Dioh W, Tharreau D, Notteghem JL, Orbach M, Lebrun M-H. 2000. Mapping of Avirulence
1087 Genes in the Rice Blast Fungus, *Magnaporthe grisea* , with RFLP and RAPD
1088 Markers. *MPMI* 13:217–227.

1089 Dong Y, Li Y, Zhao M, Jing M, Liu X, Liu M, Guo X, Zhang X, Chen Y, Liu Yongfeng, et
1090 al. 2015. Global Genome and Transcriptome Analyses of Magnaporthe oryzae
1091 Epidemic Isolate 98-06 Uncover Novel Effectors and Pathogenicity-Related Genes,
1092 Revealing Gene Gain and Lose Dynamics in Genome Evolution.Lin X, editor. *PLoS*
1093 *Pathog* 11:e1004801.

1094 Donovan DA, Crandall JG, Truong VN, Vaaler AL, Bailey TB, Dinwiddie D, Banks OG,
1095 McKnight LE, McKnight JN. 2021. Basis of specificity for a conserved and
1096 promiscuous chromatin remodeling protein. *eLife* 10:e64061.

1097 Du H, Zhang L, Liu L, Tang X-F, Yang W-J, Wu Y-M, Huang Y-B, Tang Y-X. 2009.
1098 Biochemical and Molecular Characterization of Plant MYB Transcription Factor
1099 Family. *Biochemistry Moscow* 74:1–11.

1100 Dubos C, Stracke R, Grotewold E, Weisshaar B, Martin C, Lepiniec L. 2010. MYB
1101 Transcription Factors in *Arabidopsis*. *Trends in Plant Science* 15:573–581.

1102 Erdel F, Rippe K. 2011. Binding kinetics of human ISWI chromatin-remodelers to DNA
1103 repair sites elucidate their target location mechanism. *Nucleus* 2:105–112.

1104 Erdel F, Schubert T, Marth C, Längst G, Rippe K. 2010. Human ISWI chromatin-remodeling
1105 complexes sample nucleosomes via transient binding reactions and become
1106 immobilized at active sites. *Proc. Natl. Acad. Sci. U.S.A.* 107:19873–19878.

1107 Faino L, Seidl MF, Shi-Kunne X, Pauper M, Van Den Berg GCM, Wittenberg AHJ, Thomma
1108 BPHJ. 2016. Transposons passively and actively contribute to evolution of the two-
1109 speed genome of a fungal pathogen. *Genome Res.* 26:1091–1100.

1110 Fazzio TG, Gelbart ME, Tsukiyama T. 2005. Two Distinct Mechanisms of Chromatin
1111 Interaction by the Isw2 Chromatin Remodeling Complex In Vivo. *Mol Cell Biol*
1112 25:9165–9174.

1113 Feurtey A, Lorrain C, McDonald MC, Milgate A, Solomon PS, Warren R, Puccetti G, Scalliet
1114 G, Torriani SFF, Gout L, et al. 2023. A thousand-genome panel retraces the global
1115 spread and adaptation of a major fungal crop pathogen. *Nat Commun* 14:1059.

1116 Fijarczyk A, Hessenauer P, Hamelin RC, Landry CR. 2022. Lifestyles shape genome size and
1117 gene content in fungal pathogens. Available from:
1118 http://biorxiv.org/lookup/doi/10.1101/2022.08.24.505148

1119 Flor HH. 1956. The Complementary Genic Systems in Flax and Flax Rust. In: Advances in
1120 Genetics. Vol. 8. Elsevier. p. 29–54. Available from:
1121 https://linkinghub.elsevier.com/retrieve/pii/S0065266008604988

1122 Ganapathiraju MK, Subramanian S, Chaparala S, Karunakaran KB. 2020. A reference catalog
1123 of DNA palindromes in the human genome and their variations in 1000 Genomes.
1124 *Hum Genome Var* 7:40.

1125 Hada A, Hota SK, Luo J, Lin Y, Kale S, Shaytan AK, Bhardwaj SK, Persinger J, Ranish J,
1126 Panchenko AR, et al. 2019. Histone Octamer Structure Is Altered Early in ISW2 ATP-
1127 Dependent Nucleosome Remodeling. *Cell Reports* 28:282-294.e6.

1128 Hammer O, Harper DAT, Ryan PD. 2001. PAST: Paleontological Statistics Software Package
1129 for Education and Data Analysis. 4:9.

1130 van Holde KE. 1989. Chromatin. New York, NY: Springer New York Available from:
1131 http://link.springer.com/10.1007/978-1-4612-3490-6

1132 Hopfner K-P, Gerhold C-B, Lakomek K, Wollmann P. 2012. Swi2/Snf2 remodelers: hybrid
1133 views on hybrid molecular machines. *Current Opinion in Structural Biology* 22:225–
1134 233.

1135 Hota SK, Bartholomew B. 2011. Diversity of operation in ATP-dependent chromatin
1136 remodelers. *Biochimica et Biophysica Acta (BBA) - Gene Regulatory Mechanisms*
1137 1809:476–487.

1138 Huang L, Li X, Dong L, Wang B, Pan L. 2021. Profiling of chromatin accessibility identifies
1139 transcription factor binding sites across the genome of Aspergillus species. *BMC Biol*
1140 19:189.

1141 Ipcho S, Sundelin T, Erbs G, Kistler HC, Newman M-A, Olsson S. 2016. Fungal innate
1142 immunity induced by bacterial microbe-associated molecular patterns (MAMPs). *G3*
1143 6:1585–1595.

1144 Jones JDG, Dangl JL. 2006. The plant immune system. *Nature* 444:323–329.

1145 Josefsen L, Droce A, Sondergaard TE, Sørensen JL, Bormann J, Schäfer W, Giese H, Olsson
1146 S. 2012. Autophagy provides nutrients for nonassimilating fungal structures and is
1147 necessary for plant colonization but not for infection in the necrotrophic plant
1148 pathogen Fusarium graminearum. *Autophagy* 8:326–337.

1149 Kagalwala MN, Glaus BJ, Dang W, Zofall M, Bartholomew B. 2004. Topography of the
1150 ISW2–nucleosome complex: insights into nucleosome spacing and chromatin
1151 remodeling. *EMBO J* 23:2092–2104.

1152 Kim Y, Kim H, Son H, Choi GJ, Kim J-C, Lee Y-W. 2014. MYT3, A Myb-Like
1153 Transcription Factor, Affects Fungal Development and Pathogenicity of Fusarium
1154 graminearum.Yu J-H, editor. *PLoS ONE* 9:e94359.

1155 Klevecz RR, Bolen J, Forrest G, Murray DB. 2004. A genomewide oscillation in transcription
1156 gates DNA replication and cell cycle. *Proceedings of the National Academy of*
1157 *Sciences* 101:1200–1205.

1158 Kou Y, Qiu J, Tao Z. 2019. Every Coin Has Two Sides: Reactive Oxygen Species during
1159 Rice–*Magnaporthe oryzae* Interaction. *IJMS* 20:1191.

1160 Kremer SC, Linquist S, Saylor B, Elliott TA, Gregory TR, Cottenie K. 2020. Transposable
1161 element persistence via potential genome-level ecosystem engineering. *BMC*
1162 *Genomics* 21:367.

1163 Li H, Lu J, Liu X, Xhang L, Lin F. 2012. Vector Building and Usage for Gene Knockout,
1164 Protein Expression and Fluorescent Fusion Protein in The Rice Blast Fungus. *Journal*
1165 *of Agricultural Biotechnology* 20:94–104.

1166 Li J, Han G, Sun C, Sui N. 2019. Research Advances of MYB Transcription Factors in Plant
1167 Stress Resistance and Breeding. *Plant Signaling & Behavior* 14:1613131.

1168 Li Y, Gong H, Wang P, Zhu Y, Peng H, Cui Y, Li H, Liu J, Wang Z. 2021. The emerging role
1169 of ISWI chromatin remodeling complexes in cancer. *J Exp Clin Cancer Res* 40:346.

1170 Li Y, Liang S, Yan X, Wang H, Li D, Soanes DM, Talbot NJ, Wang Zonghua, Wang
1171 Zhengyi. 2010. Characterization of *MoLDB1* Required for Vegetative Growth,
1172 Infection-Related Morphogenesis, and Pathogenicity in the Rice Blast Fungus
1173 *Magnaporthe oryzae*. *MPMI* 23:1260–1274.

1174 Li Y, Yan X, Wang H, Liang S, Ma W-B, Fang M-Y, Talbot NJ, Wang Z-Y. 2010. MoRic8 Is
1175 a Novel Component of G-Protein Signaling During Plant Infection by the Rice Blast
1176 Fungus *Magnaporthe oryzae*. *MPMI* 23:317–331.

1177 Li Y, Yue X, Que Y, Yan X, Ma Z, Talbot NJ, Wang Z. 2014. Characterisation of Four LIM
1178 Protein-Encoding Genes Involved in Infection-Related Development and

1179 Pathogenicity by the Rice Blast Fungus Magnaporthe oryzae.Xue C, editor. *PLoS*
1180 *ONE* 9:e88246.

1181 Li Y, Zheng X, Pei M, Chen M, Zhang S, Liang C, Gao L, Huang P, Olsson S. 2024.
1182 Functional Analysis of MoMyb13, a Myb Transcription Factor Involved in Regulating
1183 Growth, Conidiation, Hydrophobicity, and Pathogenicity of Magnaporthe oryzae.
1184 *Agronomy* 14:251.

1185 Li Y, Zheng X, Zhu M, Chen M, Zhang S, He F, Chen X, Lv J, Pei M, Zhang Ye, et al. 2019.
1186 MoIVD-Mediated Leucine Catabolism Is Required for Vegetative Growth,
1187 Conidiation and Full Virulence of the Rice Blast Fungus Magnaporthe oryzae. *Front.*
1188 *Microbiol.* 10:444.

1189 Lin Y, Son H, Lee J, Min K, Choi GJ, Kim J-C, Lee Y-W. 2011. A Putative Transcription
1190 Factor MYT1 Is Required for Female Fertility in the Ascomycete Gibberella zeae.Yu
1191 J-H, editor. *PLoS ONE* 6:e25586.

1192 Lin Y, Son H, Min K, Lee J, Choi GJ, Kim J-C, Lee Y-W. 2012. A Putative Transcription
1193 Factor MYT2 Regulates Perithecium Size in the Ascomycete Gibberella zeae.Yu J-H,
1194 editor. *PLoS ONE* 7:e37859.

1195 Linheiro RS, Bergman CM. 2008. Testing the palindromic target site model for DNA
1196 transposon insertion using the Drosophila melanogaster P-element. *Nucleic Acids*
1197 *Research* 36:6199–6208.

1198 Liu J, Osbourn A, Ma P. 2015. MYB Transcription Factors as Regulators of Phenylpropanoid
1199 Metabolism in Plants. *Molecular Plant* 8:689–708.

1200 Ma D, Constabel CP. 2019. MYB Repressors as Regulators of Phenylpropanoid Metabolism
1201 in Plants. *Trends in Plant Science* 24:275–289.

1202 Machné R, Murray DB. 2012. The Yin and Yang of Yeast Transcription: Elements of a
1203 Global Feedback System between Metabolism and Chromatin.Saks V, editor. *PLoS*
1204 *ONE* 7:e37906.

1205 Mateos L, Jiménez A, Revuelta JL, Santos MA. 2006. Purine Biosynthesis, Riboflavin
1206 Production, and Trophic-Phase Span Are Controlled by a Myb-Related Transcription
1207 Factor in the Fungus *Ashbya gossypii*. *Appl Environ Microbiol* 72:5052–5060.

1208 Matheis S, Yemelin A, Scheps D, Andresen K, Jacob S, Thines E, Foster AJ. 2017. Functions
1209 of the Magnaporthe oryzae Flb3p and Flb4p transcription factors in the regulation of
1210 conidiation. *Microbiological Research* 196:106–117.

1211 Menardo F, Praz CR, Wicker T, Keller B. 2017. Rapid turnover of effectors in grass powdery
1212 mildew (Blumeria graminis). *BMC Evol Biol* 17:223.

1213 Mitra P. 2018. Transcription Regulation of MYB: a Potential and Novel Therapeutic Target in
1214 Cancer. *Ann. Transl. Med* 6:443–443.

1215 Mittal P, Roberts CWM. 2020. The SWI/SNF complex in cancer — biology, biomarkers and
1216 therapy. *Nat Rev Clin Oncol* 17:435–448.

1217 Monroe JG, Srikant T, Carbonell-Bejerano P, Becker C, Lensink M, Exposito-Alonso M,
1218 Klein M, Hildebrandt J, Neumann M, Kliebenstein D, et al. 2022. Mutation bias
1219 reflects natural selection in Arabidopsis thaliana. *Nature* 602:101–105.

1220 Nürnberger T, Brunner F, Kemmerling B, Piater L. 2004. Innate immunity in plants and
1221 animals: striking similarities and obvious differences. *Immunological Reviews*
1222 198:249–266.

1223 Packer MS, Liu DR. 2015. Methods for the directed evolution of proteins. *Nat Rev Genet*
1224 16:379–394.

1225 Palloix A, Ayme V, Moury B. 2009. Durability of plant major resistance genes to pathogens
1226 depends on the genetic background, experimental evidence and consequences for
1227 breeding strategies. *New Phytologist* 183:190–199.

1228 Pattabiraman DR, Gonda TJ. 2013. Role and Potential for Therapeutic targeting of MYB in
1229 Leukemia. *Leukemia* 27:269–277.

1230 Pfeiffer T, Morley A. 2014. An evolutionary perspective on the Crabtree effect. *Front. Mol.*
1231 *Biosci.* [Internet] 1. Available from:
1232 http://journal.frontiersin.org/article/10.3389/fmolb.2014.00017/abstract

1233 Piontkivska H, Rooney AP, Nei M. 2002. Purifying Selection and Birth-and-death Evolution
1234 in the Histone H4 Gene Family. *Molecular Biology and Evolution* 19:689–697.

1235 Priebe S, Kreisel C, Horn F, Guthke R, Linde J. 2015. FungiFun2: a comprehensive online
1236 resource for systematic analysis of gene lists from fungal species. *Bioinformatics*
1237 31:445–446.

1238 Prouse MB, Campbell MM. 2012. The Interaction Between MYB Proteins and their Target
1239 DNA binding Sites. *Biochimica et Biophysica Acta (BBA) - Gene Regulatory*
1240 *Mechanisms* 1819:67–77.

1241 Rajarammohan S. 2021. Redefining Plant-Necrotroph Interactions: The Thin Line Between
1242 Hemibiotrophs and Necrotrophs. *Front. Microbiol.* 12:673518.

1243 Reisman D, Glaros S, Thompson EA. 2009. The SWI/SNF complex and cancer. *Oncogene*
1244 28:1653–1668.

1245 Roy S. 2016. Function of MYB Domain Transcription Factors in Abiotic Stress and
1246 Epigenetic Control of Stress Response in Plant Genome. *Plant Signaling & Behavior*
1247 11:e1117723.

1248 Serrano L, Vazquez BN, Tischfield J. 2013. Chromatin structure, pluripotency and
1249 differentiation. *Exp Biol Med (Maywood)* 238:259–270.

1250 Song Z, Bakeer W, Marshall JW, Yakasai AA, Khalid RM, Collemare J, Skellam E, Tharreau
1251 D, Lebrun M-H, Lazarus CM, et al. 2015. Heterologous expression of the avirulence
1252 gene ACE1 from the fungal rice pathogen Magnaporthe oryzae. *Chem. Sci.* 6:4837–
1253 4845.

1254 Stanton KA, Edger PP, Puzey JR, Kinser T, Cheng P, Vernon DM, Forsthoefel NR, Cooley
1255 AM. 2017. A Whole-Transcriptome Approach to Evaluating Reference Genes for
1256 Quantitative Gene Expression Studies: A Case Study in *Mimulus*. *G3*
1257 *Genes|Genomes|Genetics* 7:1085–1095.

1258 Svetec Miklenić M, Svetec IK. 2021. Palindromes in DNA—A Risk for Genome Stability and
1259 Implications in Cancer. *IJMS* 22:2840.

1260 Toyotome T, Kamei K. 2021. In Vitro Assay of Translation Inhibition by Trichothecenes
1261 Using a Commercially Available System. *Toxins* 13:696.

1262 Tsukiyama T, Palmer J, Landel CC, Shiloach J, Wu C. 1999. Characterization of the Imitation
1263 Switch subfamily of ATP-dependent chromatin-remodeling factors in Saccharomyces
1264 cerevisiae. *Genes & Development* 13:686–697.

1265 Valsecchi I, Sarikaya-Bayram Ö, Wong Sak Hoi J, Muszkieta L, Gibbons J, Prevost M-C,
1266 Mallet A, Krijnse-Locker J, Ibrahim-Granet O, Mouyna I, et al. 2017. MybA, a
1267 transcription factor involved in conidiation and conidial viability of the human
1268 pathogen *Aspergillus fumigatus*: A transcription factor regulating conidiation in
1269 *Aspergillus*. *Molecular Microbiology* 105:880–900.

1270 Verma S, Gazara RK, Verma PK. 2017. Transcription Factor Repertoire of Necrotrophic
1271 Fungal Phytopathogen *Ascochyta rabiei*: Predominance of MYB Transcription Factors
1272 As Potential Regulators of Secretome. *Front. Plant Sci.* 8:1037.

1273 Villalba F, Collemare J, Landraud P, Lambou K, Brozek V, Cirer B, Morin D, Bruel C, Beffa
1274 R, Lebrun M-H. 2008. Improved gene targeting in Magnaporthe grisea by inactivation
1275 of MgKU80 required for non-homologous end joining. *Fungal Genetics and Biology*
1276 45:68–75.

1277 Wang X, Angelis N, Thein SL. 2018. MYB – A regulatory Factor in Hematopoiesis. *Gene*
1278 665:6–17.

1279 Whitehouse I, Rando OJ, Delrow J, Tsukiyama T. 2007. Chromatin remodelling at promoters
1280 suppresses antisense transcription. *Nature* 450:1031–1035.

1281 Wieser J, Adams TH. 1995. *fibD* encodes a Myb-like DNA-binding protein that coordinates
1282 initiation of *Aspergillus mdulans* conidiophore development. *Genes & Development*
1283 9:491–502.

1284 Willcockson MA, Healton SE, Weiss CN, Bartholdy BA, Botbol Y, Mishra LN, Sidhwani
1285 DS, Wilson TJ, Pinto HB, Maron MI, et al. 2021. H1 histones control the epigenetic
1286 landscape by local chromatin compaction. *Nature* 589:293–298.

1287 Yoshida K, Saunders DGO, Mitsuoka C, Natsume S, Kosugi S, Saitoh H, Inoue Y, Chuma I,
1288 Tosa Y, Cano LM, et al. 2016. Host specialization of the blast fungus Magnaporthe
1289 oryzae is associated with dynamic gain and loss of genes linked to transposable
1290 elements. *BMC Genomics* 17:370.

1291 Zhang L, Zhang D, Chen Y, Ye W, Lin Q, Lu G, Ebbole DJ, Olsson S, Wang Z. 2019.
1292 *Magnaporthe oryzae* CK2 Accumulates in Nuclei, Nucleoli, at Septal Pores and

1293 Forms a Large Ring Structure in Appressoria, and Is Involved in Rice Blast
1294 Pathogenesis. *Frontiers in Cellular and Infection Microbiology* 9:113.

1295 Zhang L, Zhang D, Liu D, Li Y, Li H, Xie Y, Wang Z, Hansen BO, Olsson S. 2019.
1296 Conserved Eukaryotic Kinase CK2 Chaperone Intrinsically Disordered Protein
1297 Interactions. Druzhinina IS, editor. *Appl Environ Microbiol* 86:e02191-19,
1298 /aem/86/2/AEM.02191-19.atom.

1299 Zhao C, Waalwijk C, de Wit PJ, Tang D, van der Lee T. 2014. Relocation of genes generates
1300 non-conserved chromosomal segments in Fusarium graminearum that show distinct
1301 and co-regulated gene expression patterns. *BMC Genomics* 15:191.

1302 Zofall M, Persinger J, Bartholomew B. 2004. Functional Role of Extranucleosomal DNA and
1303 the Entry Site of the Nucleosome in Chromatin Remodeling by ISW2. *Mol Cell Biol*
1304 24:10047–10057.

1305

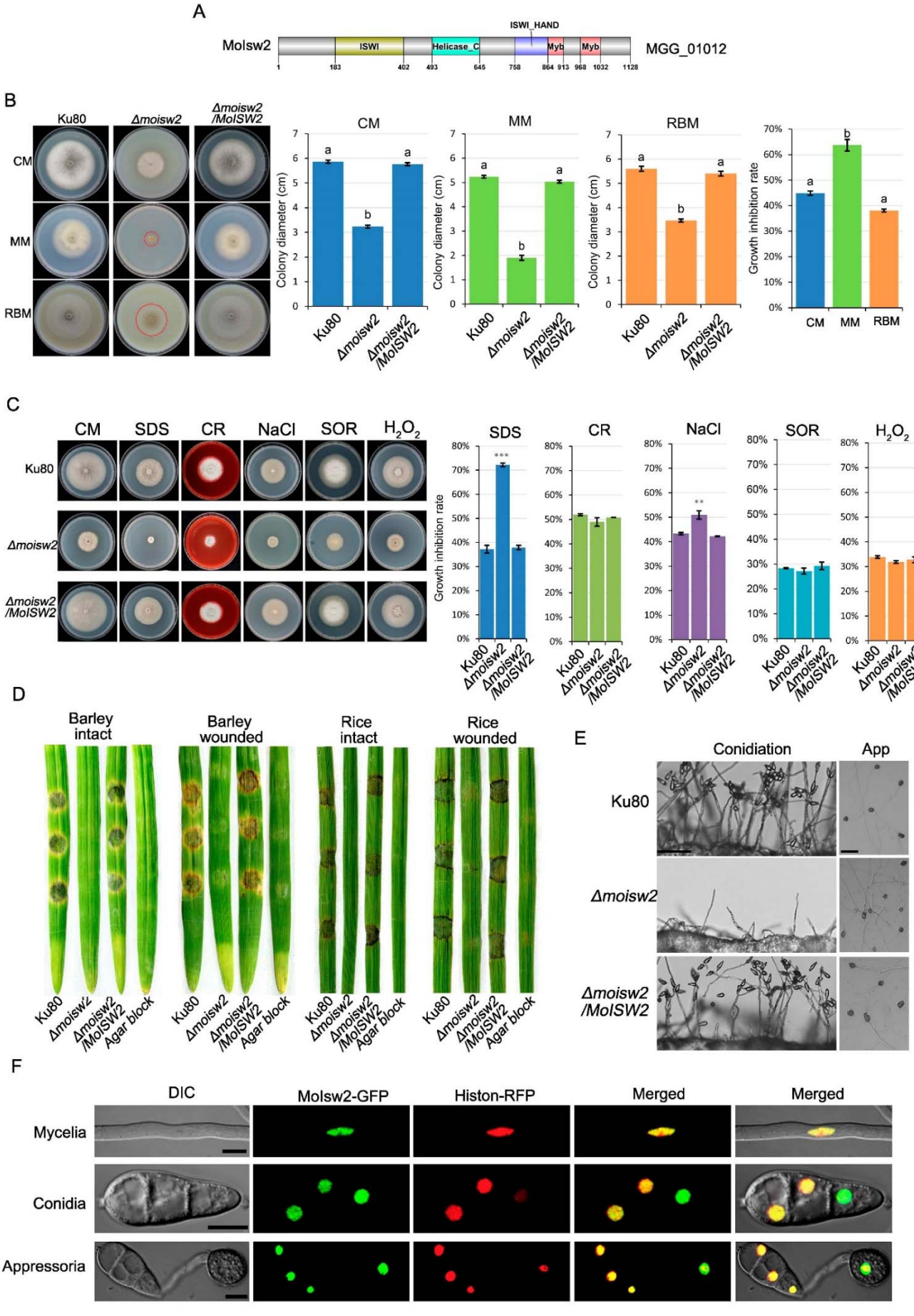

Figure 1. Domain structure, knockout phenotypes compared to the background Ku80, and localization of MoIsw2. (A) Domain structure (B) Growth phenotypes and growth on complete medium (CM) minimal medium (MM) and rice bran medium (RBM). (C) Stress phenotypes on complete medium (CM) with added Sodium Dodecyl Sulfate (SDS), Congo Red (CR), salt (NaCl), sorbitol (SOR) or hydrogen peroxide (H_2O_2). (D) Infection phenotypes on barley and rice leaves. (E) Conidia formation and appressoria formation from hyphae. (F) Subcellular localization in mycelia, conidia and appressoria MoIsw2-GFP localizes to nuclei (Histon1-RFP nuclear marker). The same letter on the bars indicates $P_{same} >$ *0.05. The stars above bars indicate significant differences from the Ku80 controls ** $P_{same} < 0.01$ ***$P_{same} < 0.001$.

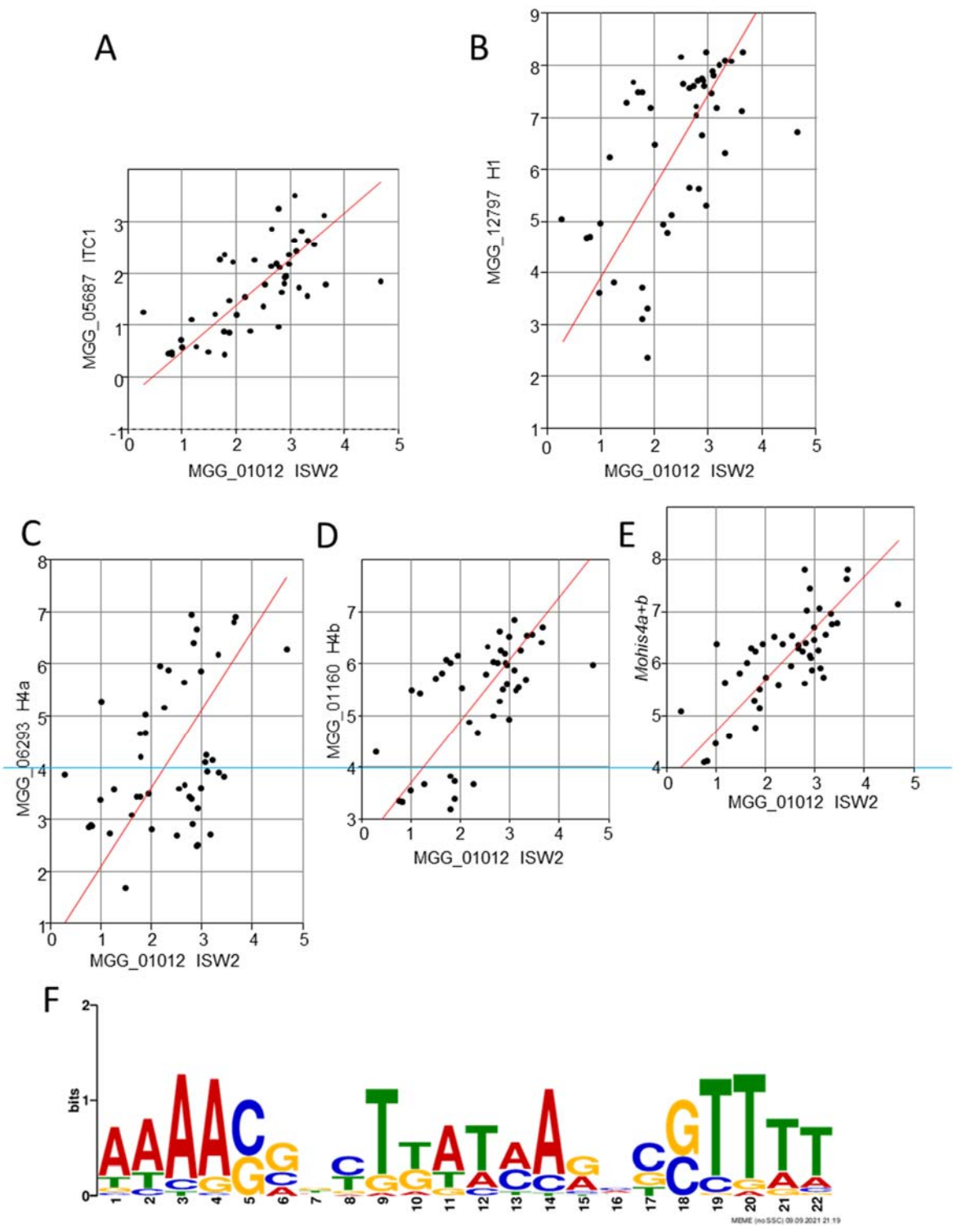

Figure 2. Log2 Reduced Major Axis (RMA) correlations of a putative *ITC1*, the linker histone *HIS1* and the two putative *HIS4* genes putatively expressing the same protein known to interact with the expression of the putative *MoISW2* (x-axis) in published RNAseq data at different stages of plant infection. Each dot represents the two genes'

expression in a separate RNAseq dataset. RMA fitting was used to handle the problem of errors in both X and Y axis values, an inherent consequence of plotting the expression of 2 genes against each other. Each dot corresponds to the value from one transcriptome. (**A**) ITC1, P(uncorrelated)=1.57E-7 (**B**) *HIS1*, P(uncorrelated)=1.48E-5 (**C**) *HIS4a* P(uncorrelated)=0.0044 (**D**) *HIS4b* P(uncorrelated)=3.81E-7 (**E**) *HIS4a* + *4b* since both *HIS4* genes are predicted to encode for the same protein, P(uncorrelated) 5.82E-10. All plots are shown with equal x and y scale gradings so that it is easy to compare slopes between graphs visually. Also, note that figures **C**, **D**, and **E** have been positioned so that Log 4 on the Y-axes are on the same line so that the effect of the addition, Log2(His4a+His4b), can be seen visually. (**F**) A frequently occurring palindromic motif was found in the ChIP-seq data using MoIsw2 as bait. It was found in 196 sequences.

Table 1. Comparison of the position of avirulence genes compared to the position of the MoIsw2 palindromic DNA binding motif sites in strain Guy11, as well as differential regulation between experiments of the avirulence genes in MoISW2 knockout compared to the background, and differential regulation of the same genes during infection of rice in strain Guy11, and strain 98-06 from published data. Blue-marked cells; are genes that MoIsw2 help regulate only in Guy11. Green-marked cells; are genes that are only regulated during infection by 98-06. DelR and VarR contain variation in expression in RNAseq data between mutant and Ku80, and between 55 downloaded RNAseq datasets from different labs, respectively (see text below for explanation of these measures). Several of the listed avirulence genes are not present in any of the two strains and some are only present in one of them.

ID.	Annotation	Distance from the closest gene to MoIsw2 binding site Guy11	DelR Guy11	Guy11 expr (X)	98-06 expr (X)	VarR Guy11
MGG_12447	cytochalasan	0	19.31	X		48.20
MGG_08386	cytochalasan	NP				
MGG_08377	cytochalasan	NP				
MGG_08378	cytochalasan	1	15.25	X		15.25
MGG_08380	cytochalasan	?			X	
MGG_08381	cytochalasan	?			X	
MGG_08384	cytochalasan	2	0.08	X	X	**29.55**
MGG_08389	cytochalasan	2	2.33	X	X	**24.59**
MGG_08390	cytochalasan	1	0.00	X	X	**56.00**
MGG_08391	cytochalasan	?			X	

MGG_15927	cytochalasan	?			X	
MGG_15928	cytochalasan	NP				

	Avirulence genes					
MGG_07199	ATR13, RxLR effector	170	0.04	X	X	7.27
MGG_10556	Avr_Pii	NP				
MGG_17614	Avr_Pii	NP				
MGG_13283	Avr_Pik	NP				
MGG_15972	Avr_Pik	?			X	
MGG_03029	Avr_Pita1	175	37.08			19.74
MGG_07038	Avr_Pita1	169	2.00			6.25
MGG_09617	Avr_Pita1	NP				
MGG_10927	Avr_Pita1	20	0.07			**24.00**
MGG_03808	Avr_Pita1 like	NP				
MGG_15370	Avr_Pita1 like	1	0.28			**56.00**
MGG_17611	Avr_Pita1	NP				
MGG_14981	AVR_PiTA2	NP				
MGG_15212	AVR_Pita2	?			X	
MGG_18041	Avr_Piz-t	NP				
MGG_03685	Avr-Pi54	238	14.11			3.86
MGG_13863	Avr-PWL1	?			X	
MGG_07398	Avr-PWL2	NP		X		
Sum number	30			7	11	
Only in one of the strains				3	7	
				In both		
				4		

NP=Not Present in Guy11 or 98-06

Bold numbers=Seem to be more important during plant infection

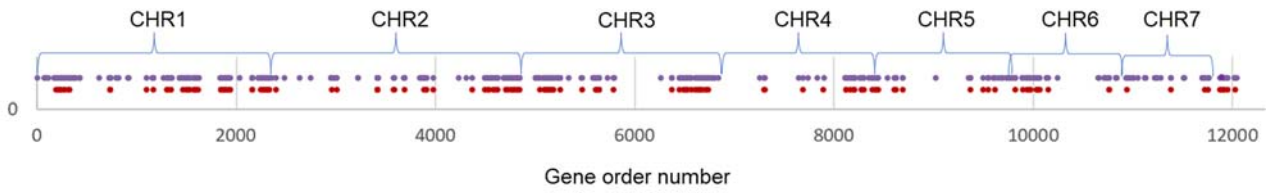

Figure 3. The position of TEs and identified palindromic MoIsw2 binding sites in DNA largely overlap along the whole genome.

Table 1. Comparison of the position of avirulence genes compared to the position of the MoIsw2 palindromic DNA binding motif sites in strain Guy11, as well as differential regulation between experiments of the avirulence genes in MoISW2 knockout compared to the background, and differential regulation of the same genes during infection of rice in strain Guy11, and strain 98-06 from published data. Blue-marked cells; are genes that MoIsw2 help regulate only in Guy11. Green-marked cells; are genes that are only regulated during infection by 98-06. DelR and VarR contain variation in expression in RNAseq data between mutant and Ku80, and between 55 downloaded RNAseq datasets from different labs, respectively (see text below for explanation of these measures). Several of the listed avirulence genes are not present in any of the two strains and some are only present in one of them.

ID.	Annotation	Distance from the closest gene to MoIsw2 binding site Guy11	DelR Guy11	Guy11 expr (X)	98-06 expr (X)	VarR Guy11
MGG_12447	cytochalasan	0	19.31	X		48.20
MGG_08386	cytochalasan	NP				
MGG_08377	cytochalasan	NP				
MGG_08378	cytochalasan	1	15.25	X		15.25
MGG_08380	cytochalasan	?			X	
MGG_08381	cytochalasan	?			X	
MGG_08384	cytochalasan	2	0.08	X	X	**29.55**
MGG_08389	cytochalasan	2	2.33	X	X	**24.59**
MGG_08390	cytochalasan	1	0.00	X	X	**56.00**
MGG_08391	cytochalasan	?			X	

MGG_15927	cytochalasan	?			X	
MGG_15928	cytochalasan	NP				

	Avirulence genes					
MGG_07199	ATR13, RxLR effector	170	0.04	X	X	7.27
MGG_10556	Avr_Pii	NP				
MGG_17614	Avr_Pii	NP				
MGG_13283	Avr_Pik	NP				
MGG_15972	Avr_Pik	?			X	
MGG_03029	Avr_Pita1	175	37.08			19.74
MGG_07038	Avr_Pita1	169	2.00			6.25
MGG_09617	Avr_Pita1	NP				
MGG_10927	Avr_Pita1	20	0.07			**24.00**
MGG_03808	Avr_Pita1 like	NP				
MGG_15370	Avr_Pita1 like	1	0.28			**56.00**
MGG_17611	Avr_Pita1	NP				
MGG_14981	AVR_PiTA2	NP				
MGG_15212	AVR_Pita2	?			X	
MGG_18041	Avr_Piz-t	NP				
MGG_03685	Avr-Pi54	238	14.11			3.86
MGG_13863	Avr-PWL1	?			X	
MGG_07398	Avr-PWL2	NP		X		
Sum number	30			7	11	
Only in one of the strains				3	7	
				In both		
				4		

NP=Not Present in Guy11 or 98-06

Bold numbers=Seem to be more important during plant infection

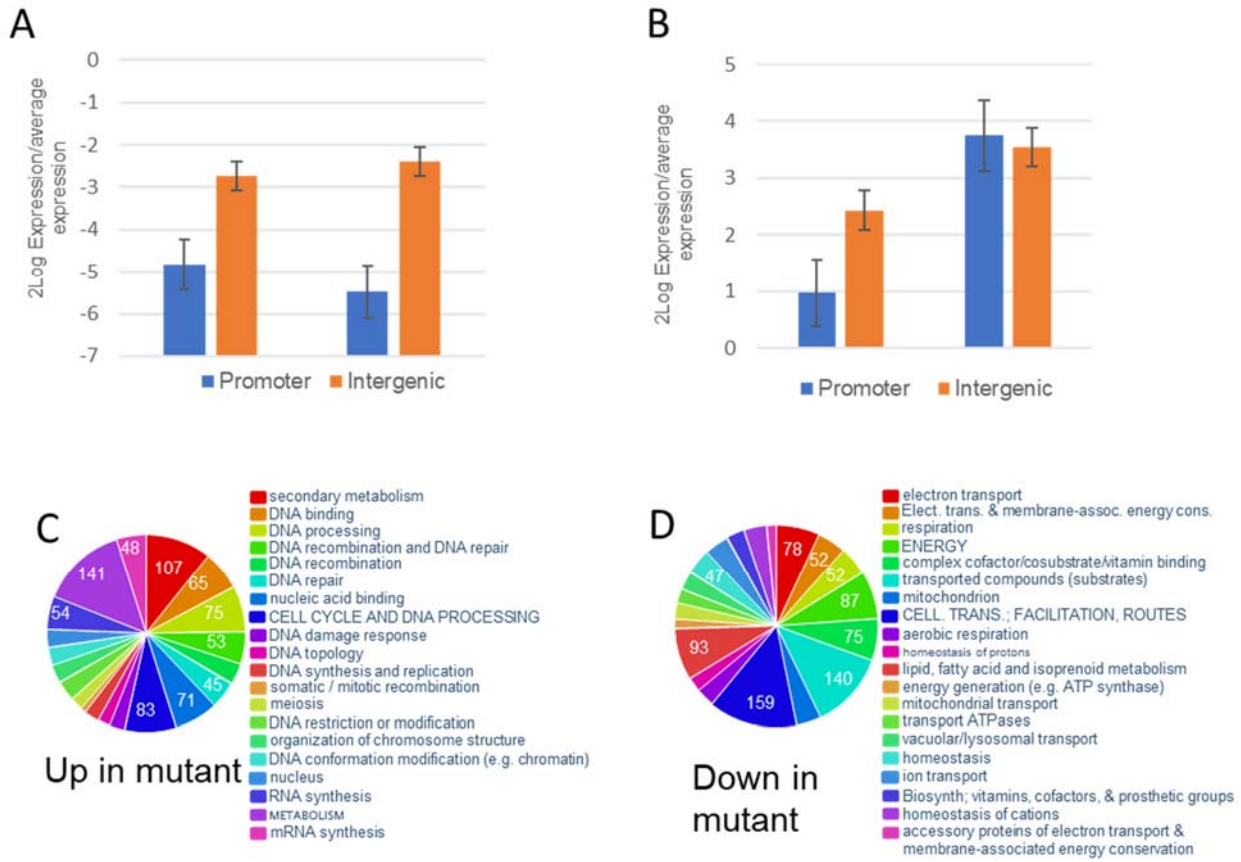

Figure 4. Deletion-induced change in expression of genes next to the predicted palindromic MoIsw2 DNA binding site with hits for the MoIsw2 binding in the ChIP-seq data compared to the average regulation of all genes. (**A**) Expression was, on average higher of genes closest to the binding site in *ΔMoISW2* than Ku80, or with the motif in their promoter region. (**B**) Expression of genes with a binding site in the promoter region and the closest gene when MoIsw2 binding is intergenic. MoIsw2 upregulates both gene types and upregulates genes slightly further away from the binding site, while the absolute (plus or minus) regulation is equal for both types of genes (8-16 times regulation). Error bars indicate SEM (Promoter N=63 Intergenic N=112). (**C**) 20 most significantly enriched upregulated FunCat gene categories in the *ΔMoISW2* compared to the background strain Ku80; Secondary metabolism, DNA-binding, and genes for DNA-related activities and synthesis (anabolism). (**D**)

20 Significantly enriched downregulated genes in the mutant are genes for, mitochondrial activities like electron transport and mitochondrial biosynthesis, respiration, and transport routes (catabolism).

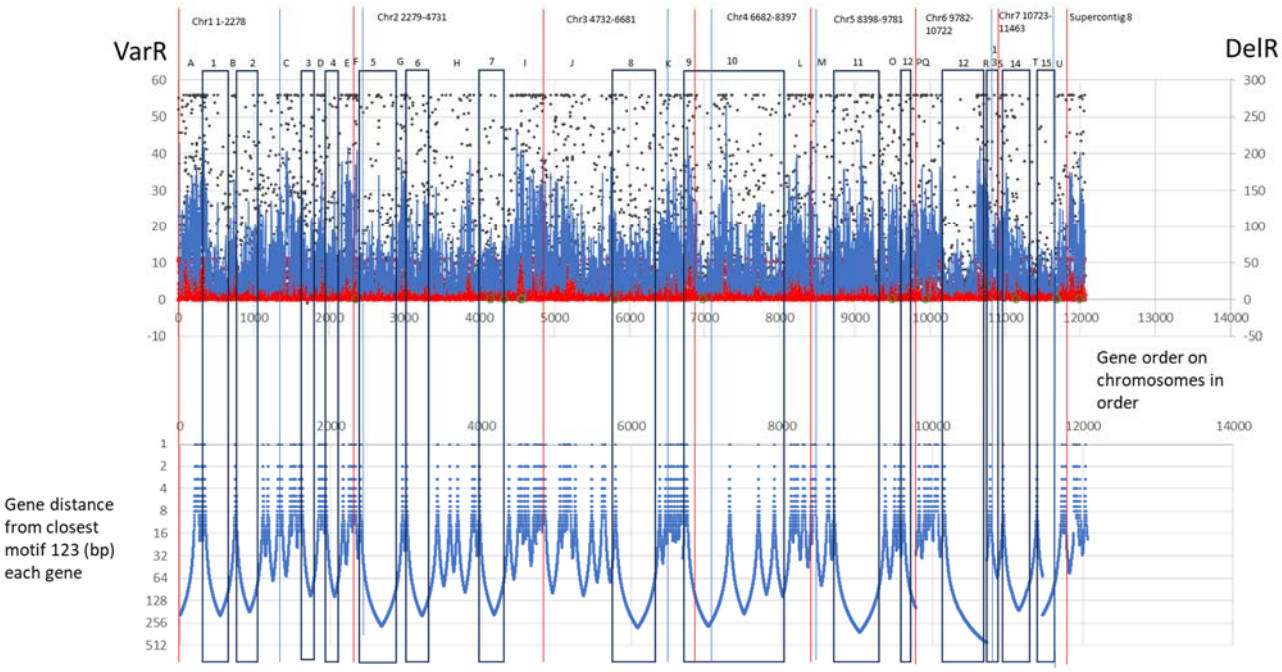

Figure 5. A plot of distances of all genes to the closest motifs of the 123 binding motifs sites (**bottom**) is compared to a plot of the variation of expression across 55 RNAseq experiments (black points and blue 5-point moving average) combined with the difference in gene expression between the *MoISW2* mutant and the Ku80 background (Red points and bright red 5-point moving average (**top**) (DelR). For the VarR data, several genes had at least one condition when their expression was below the detection level while otherwise expressed in these cases the gene expression was set to the lowest detected gene expression. That creates a line of black dots at the top of the figure. The density of the line of dots (top figure) together with areas with less than 16 gene distances from the motif sites paints out the regions of the genome with the most variation in both the VarR and DelR data. The genome contains A-U genomic regions with high variability of gene expression closest (less than 16 genes away) to the MoIsw2 123 DNA binding motifs sites and 1-15 regions with lower variation. Note bottom Y axis is log and reverse, X axis is gene order from 1->12000 on the

105 chromosomes in chromosome order from 1-7 plus supercontig 8 for the whole genome

106 to get the whole genome in order.

107

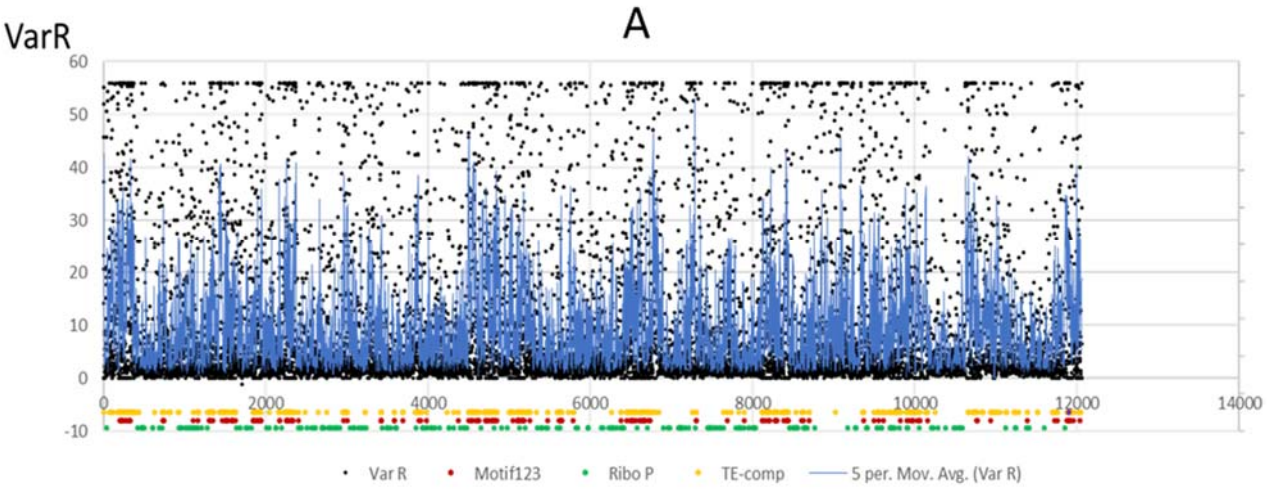

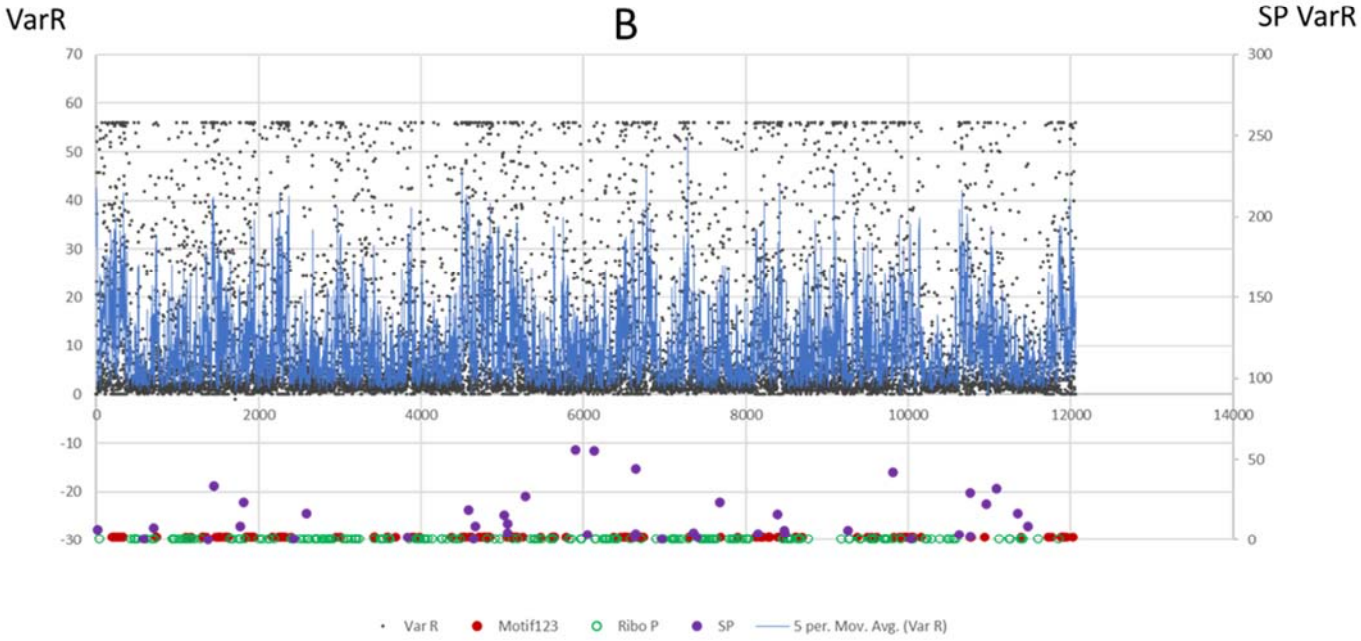

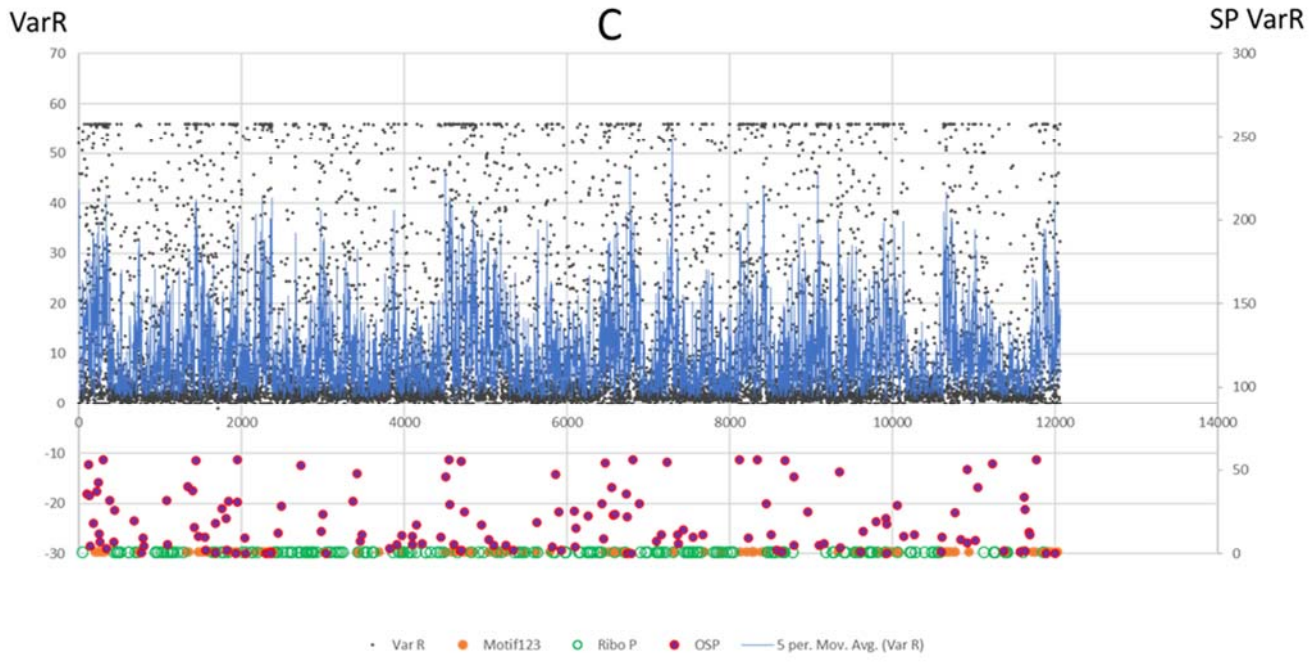

108

Figure 6. Position of housekeeping ribosomal genes and genes encoding secreted proteins compared to the position of MoIsw2 DNA binding motifs and genes encoding ribosomal genes compared to VarR variability. (**A**) Ribosomal genes. (**B**) Genes for secreted proteins (SP) with conserved domains (generally larger secreted proteins). (**C**) Genes for other secreted proteins (OSP) without any conserved domains identified (generally small secreted proteins and peptides).

116 .

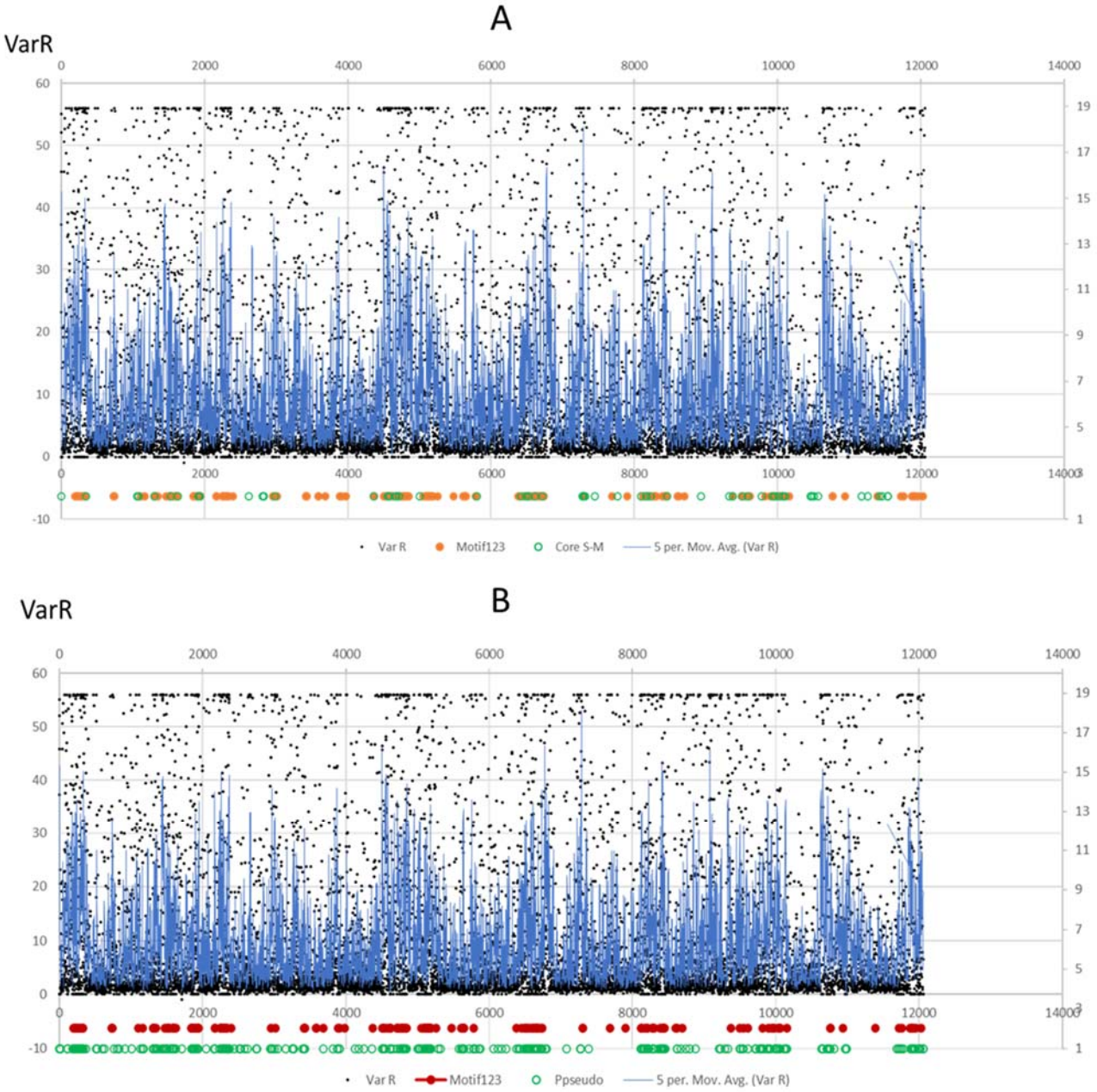

117

118 **Figure 7**. Position of core secondary metabolite genes and potential pseudogenes
119 compared to the position of the MoIsw2 DNA binding motifs and genes encoding
120 ribosomal genes compared to VarR variability. (**A**) Core secondary metabolite genes
121 (green rings). (**B**) Potential pseudogenes not expressed in any treatment (dark green
122 rings). In both A and B, the positions of the 123 MoIsw2 DNA binding motif sites are
123 marked as references.

Table 2. Annotation of the 65 DNA binding genes identified in the analysis shown in Fig. 3C. These 65 genes are the most upregulated in *ΔMoISW2* compared to the expression in the background Ku80-strain. Annotation from NCBI. Note: these are the genes that are most repressed by the MoIsw2 activity.

MGG_02762	MGG_02762. ATP-dependent RNA helicase DED1; Belongs to the DEAD box helicase family
MGG_06470	MGG_06470, DNA repair helicase RAD25 (835 aa).
MGG_05948	MGG_05948 zinc knuckle domain-containing protein. This domain is a zinc-binding domain of the form CxxCxxxGHxxxxC from various species. It is found in the MPE1 protein from Saccharomyces cerevisiae which is a component of the cleavage and polyadenylation factor (CPF) complex important for polyadenylation-dependent pre-mRNA 3'-end formation
MGG_01990	b-ZIP transcription factor IDI-4 (induces autophagic cell death in the fungus *Podospora*)
MGG_00868	Global Transactivator; Superfamily II DNA or RNA helicase, SNF2 family [Transcription, Replication, recombination and repair];
MGG_02429	KOG4062 6-O-methylguanine-DNA methyltransferase MGMT/MGT1, involved in DNA repair Replication, recombination and repair https://jgi-myco-web-4.jgi.doe.gov/annotator/servlet/jgi.annotation.Annotation?pDb=Lasov1&pStateVar=View&pProteinId=680852&pViewType=protein
MGG_07015	DNA repair protein Rad7
MGG_11518	G/U mismatch-specific uracil DNA glycosylase
MGG_04428	Zinc finger transcription factor ace1
MGG_07118	sporulation-specific protein 5 (needed for sexual spore formation?)
MGG_05995	MGG_05995, Magnaporthe oryzae 70-15 hypothetical protein (244 aa), translin family protein, Translin family (PF01997). If Translin, here is a review about that https://link.springer.com/article/10.1007/s12038-019-9947-6.
MGG_04429	ATP-dependent DNA helicase MPH1; ATP-dependent DNA helicase is involved in DNA damage repair by homologous recombination and genome maintenance.

124

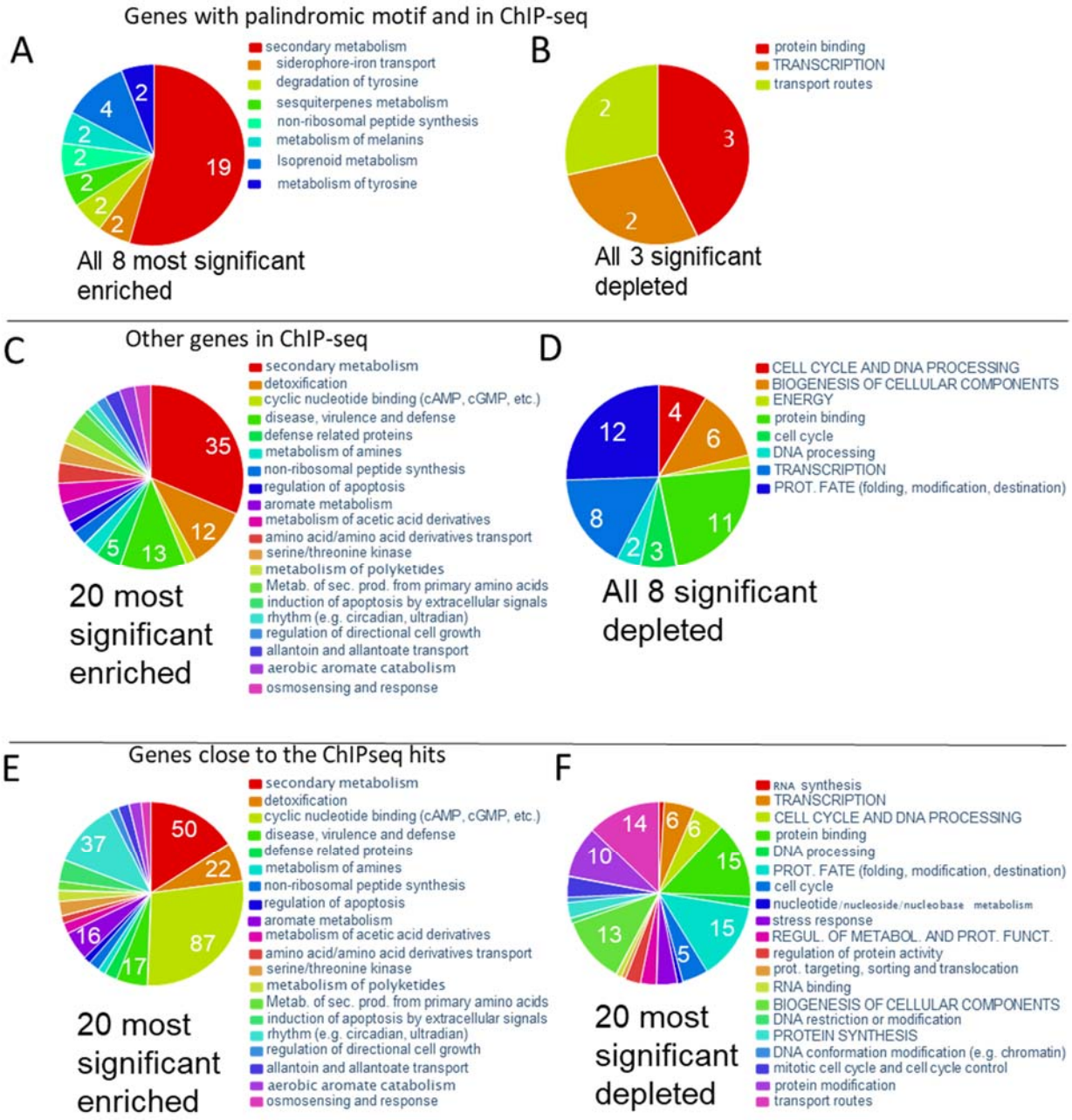

Figure 8. FunCat classification of genes at or close to the MoIsw2 DNA binding sites. (**A**) Significantly enriched and depleted classes of genes in the MoIsw2 ChIP-seq binding assay that also has the MoIsw2 DNA-binding palindromic motif in their upstream region. **(B)** Significantly enriched and depleted classes of all genes with ChIP-seq sequences with MoIsw2 binding to their upstream regulatory DNA

132 sequences. **(C)** Significantly enriched and depleted classes of genes closest to
133 intergenic hits for MoIsw2 binding, excluding the palindromic motif hits
134

135 .

136

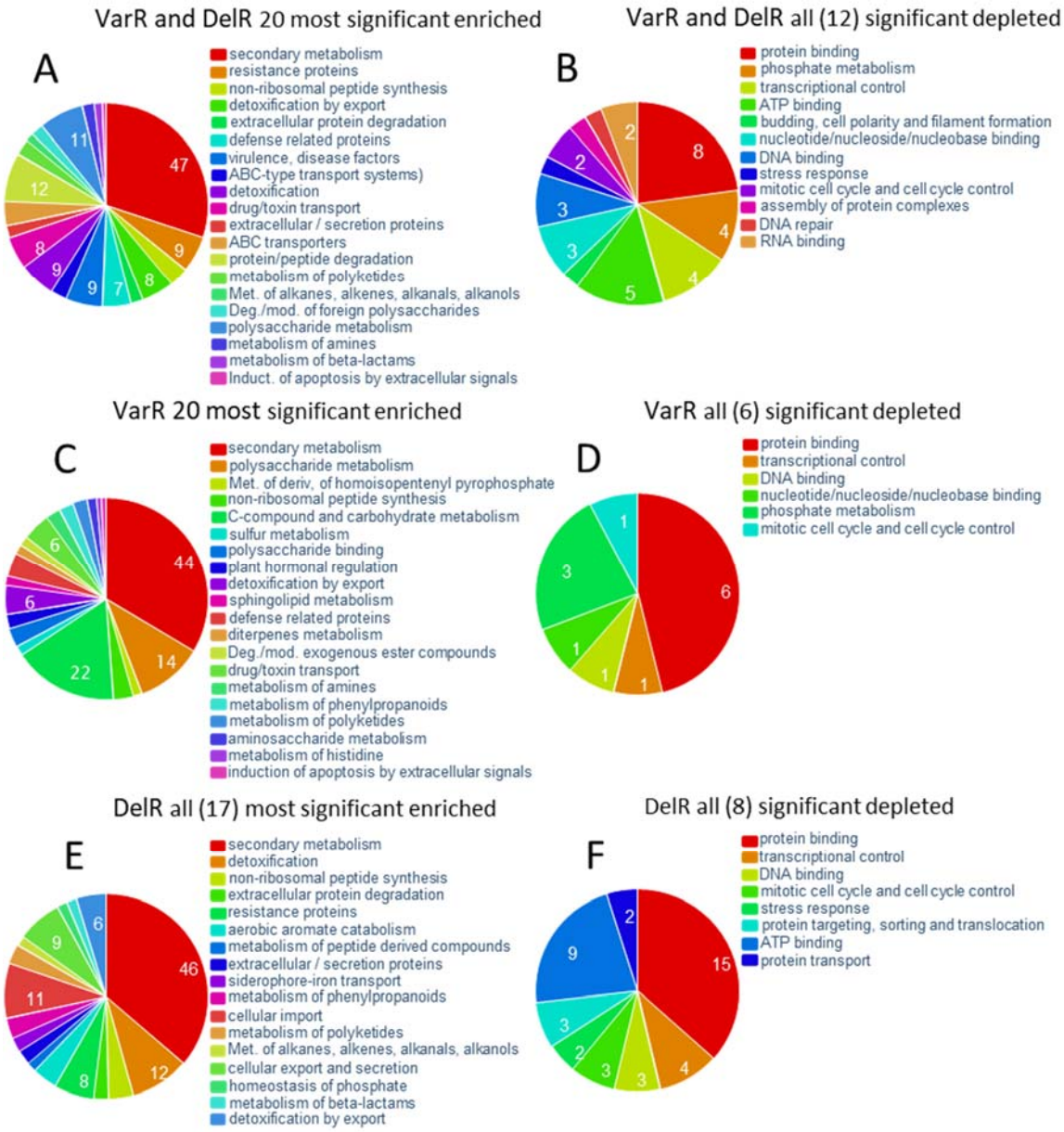

137

138

139 **Figure 9.** FunCat classification of 500 genes with the most variable gene expression

140 between experiments. (**A**) VarR and DelR enriched. (**B**) VarR and DelR depleted. (**C**)

141 VarR alone Enriched. (**D**) VarR alone depleted. (**E**) DelR alone enriched. (**F**) DelR

142 alone depleted.

143

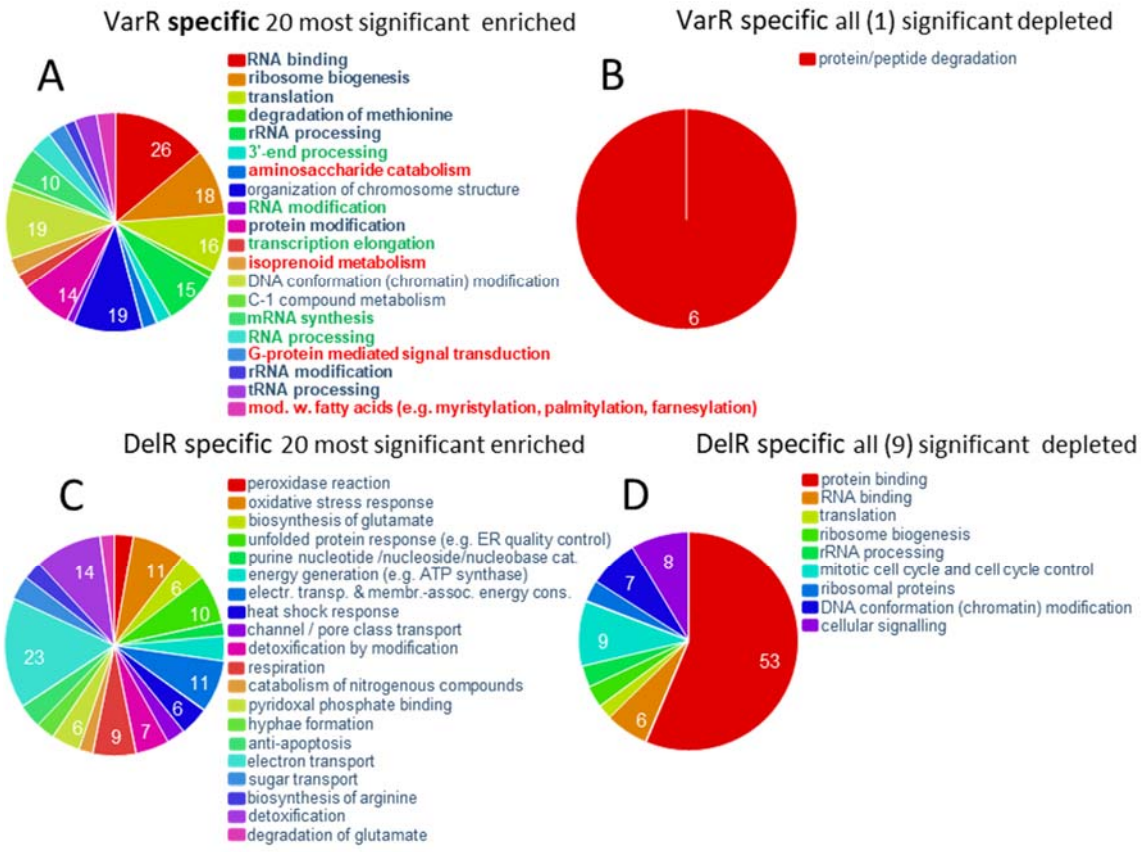

144

145 Black bold=translation related

146 Green bold=transcription related

147 Red bold=innate immunity related (towards plant? amino saccharide metabolism)

148

149 **Figure 10** Differences between 500 VarR-specific and DelR-**specific** functional gene
150 classes illustrate the difference in conditions between *in planta* experiments and *in vitro*
151 experiments. (**A**) VarR-specific significantly enriched functional gene classes
152 specifically responding *in planta*. Colour-marked texts are the functional gene classes
153 of special interest for plant pathogenicity (see text). (**B**) VarR-specific significantly
154 depleted functional gene classes specifically responding *in planta*. (**C**) DelR-specific
155 significantly enriched functional gene classes specifically responding *in vitro* (**D**)
156 DelR-specific significantly depleted functional gene classes specifically responding *in*
157 *vitro*.

Key resources table

REAGENT or RESOURCE	SOURCE	IDENTIFIER
Chemicals, peptides, and recombinant proteins		
MoISW2GFP	This paper	
Critical commercial assays		
ChIP seq service	IGENEBOOK (see this paper supplemental file)	Supplemental Company methods.zip
RNAseq service	IGENEBOOK (see this paper supplemental file)	Supplemental Company methods.zip
Deposited data		
RNAseq compilation of published experiments on gene expressions during infection stages	Zhang et al.[2]	https://doi.org/10.6084/m9.figshare.7068857.v1
ChIPsec data for MoISW2 binding M. oryzae Ku80 DNA RNAseq data for strains ΔMoIsw2 and Ku80 + other supplemental files and analyses 50Mb zip file.	This paper	https://figshare.com/s/df7b6b0bf9caf963a06c reserved DOI https://doi.org/10.6084/m9.figshare.22218328
Magnaporthe oryzae genome, genes sequences and gene contig order data needed to arrange genes in correct order on supercontigs.	BROAD institute	ftp.broadinstitute.org/distribution/annotation/fungi/magnaporthe/genomes/magnaporthe_oryzae_70-15_8 User: Anonymous
Magnaporth oryzae expression Avir genes during rice infection. Strain 98-06	Cao et al. [3]	https://bsppjournals.onlinelibrary.wiley.com/action/downloadSupplement?doi=10.1111%2Fmpp.13224&file=mpp13224-sup-0010-TableS2.xlsx
Sequence downloads, blasts, annotations including domain annotations	NCBI	https://www.ncbi.nlm.nih.gov/
Experimental models: Organisms/strains		
Magnaporthe oryzae (formerly *Magnaporthe grisea*)		Ku80[4] deletion in strain Guy11 NCBI:txid242507
MoISW2-GFP strain derived from Ku80	Li et al. [1]	https://doi.org/10.1101/2021.12.28.474317
Software and algorithms		
PAST statistics software package version 4.08 (released November 2021)	Hammer et al.[5]	https://www.nhm.uio.no/english/research/infrastructure/past/

Microsoft Excel (MS office 365) with Solver Add-In activated	Microsoft	https://www.microsoft.com
Fisher Exact Add-In for MS Excel	software@obertfamily.com	http://www.obertfamily.com/software/fisherexact.html
Other		
FungiFun2 website for Functional Category analysis of putative proteins.	Priebe et al. [6]	https://elbe.hki-jena.de/fungifun/fungifun.php
antiSMASH website for finding core secondary metabolite genes in fungi.	Blin et al. [7]	https://fungismash.secondarymetabolites.org/#!/start
The MEME suite for use of MEME and FIMO	Bailey et al. [8]	https://meme-suite.org/meme/

1. Li, Y. *et al. The* Myb *family genes in the rice pathogen* Magnaporthe oryzae *: Finding and deleting more family members involved in pathogenicity*. http://biorxiv.org/lookup/doi/10.1101/2021.12.28.474317 (2021) doi:10.1101/2021.12.28.474317.
2. Zhang, L. *et al.* Conserved Eukaryotic Kinase CK2 Chaperone Intrinsically Disordered Protein Interactions. *Appl Environ Microbiol* **86**, e02191-19, /aem/86/2/AEM.02191-19.atom (2019).
3. Cao, Y. *et al.* Characterization of two infection-induced transcription factors of *Magnaporthe oryzae* reveals their roles in regulating early infection and effector expression. *Molecular Plant Pathology* **23**, 1200–1213 (2022).
4. Villalba, F. *et al.* Improved gene targeting in Magnaporthe grisea by inactivation of MgKU80 required for non-homologous end joining. *Fungal Genetics and Biology* **45**, 68–75 (2008).
5. Hammer, O., Harper, D. A. T. & Ryan, P. D. PAST: Paleontological Statistics Software Package for Education and Data Analysis. **4**, 9 (2001).
6. Priebe, S., Kreisel, C., Horn, F., Guthke, R. & Linde, J. FungiFun2: a comprehensive online resource for systematic analysis of gene lists from fungal species. *Bioinformatics* **31**, 445–446 (2015).
7. Blin, K. *et al.* antiSMASH 6.0: improving cluster detection and comparison capabilities. *Nucleic Acids Research* **49**, W29–W35 (2021).
8. Bailey, T. L., Johnson, J., Grant, C. E. & Noble, W. S. The MEME Suite. *Nucleic Acids Res* **43**, W39–W49 (2015).